NAVAL POSTGRADUATE SCHOOL
Monterey, California

THESIS

LOITERING BEHAVIORS OF AUTONOMOUS UNDERWATER VEHICLES

by

Douglas L. Williams

June 2002

Thesis Advisor: Anthony J. Healey

Approved for public release; distribution is unlimited.

THIS PAGE INTENTIONALLY LEFT BLANK

REPORT DOCUMENTATION PAGE			Form Approved OMB No. 0704-0188
Public reporting burden for this collection of information is estimated to average 1 hour per response, including the time for reviewing instruction, searching existing data sources, gathering and maintaining the data needed, and completing and reviewing the collection of information. Send comments regarding this burden estimate or any other aspect of this collection of information, including suggestions for reducing this burden, to Washington headquarters Services, Directorate for Information Operations and Reports, 1215 Jefferson Davis Highway, Suite 1204, Arlington, VA 22202-4302, and to the Office of Management and Budget, Paperwork Reduction Project (0704-0188) Washington DC 20503.			
1. AGENCY USE ONLY ***(Leave blank)***	**2. REPORT DATE** June 2002	**3. REPORT TYPE AND DATES COVERED** Master's Thesis	
4. TITLE AND SUBTITLE: Loitering Behaviors of Autonomous Underwater Vehicles			**5. FUNDING NUMBERS**
6. AUTHOR(S) Douglas L. Williams			
7. PERFORMING ORGANIZATION NAME(S) AND ADDRESS(ES) Naval Postgraduate School Monterey, CA 93943-5000			**8. PERFORMING ORGANIZATION REPORT NUMBER**
9. SPONSORING / MONITORING AGENCY NAME(S) AND ADDRESS(ES) N/A			**10. SPONSORING / MONITORING AGENCY REPORT NUMBER**
11. SUPPLEMENTARY NOTES The views expressed in this thesis are those of the author and do not reflect the official policy or position of the Department of Defense or the U.S. Government.			
12a. DISTRIBUTION / AVAILABILITY STATEMENT Approved for public release; distribution is unlimited.			**12b. DISTRIBUTION CODE**

13. ABSTRACT

In multi-vehicle mine hunting operations, it will be necessary at times for one vehicle to loiter at some point while gathering communications of data from other vehicles. The loitering behaviors of the ARIES Autonomous Underwater Vehicle have never been completely defined. The track that the vehicle chooses to maintain station while circling around one specific point for an extended period of time may be sometimes random and unpredictable, unless defined in terms of specific tracks. Simulations were run and analyzed for various conditions to record the tendencies of the vehicle during different current conditions and approach situations. The stability of the Heading Controller was then analyzed in order to predict the position where the Line of Sight Guidance algorithm becomes unstable. The data obtained through the simulations supports and explains the tendencies ARIES exhibits while circling around a loiter point.

14. SUBJECT TERMS: Autonomous Underwater Vehicles, Robotics, Loitering Behavior, Line of Sight Guidance Instability, Liapunov Stability/Instability Theorem			**15. NUMBER OF PAGES** 72
			16. PRICE CODE
17. SECURITY CLASSIFICATION OF REPORT Unclassified	**18. SECURITY CLASSIFICATION OF THIS PAGE** Unclassified	**19. SECURITY CLASSIFICATION OF ABSTRACT** Unclassified	**20. LIMITATION OF ABSTRACT** UL

NSN 7540-01-280-5500 Standard Form 298 (Rev. 2-89)
Prescribed by ANSI Std. 239-18

THIS PAGE INTENTIONALLY LEFT BLANK

Approved for public release; distribution is unlimited.

LOITERING BEHAVIOR OF AUTONOMOUS UNDERWATER VEHICLES

Douglas L. Williams
Lieutenant, United States Navy
B.S., United States Naval Academy, 1995

Submitted in partial fulfillment of the
requirements for the degree of

MASTER OF SCIENCE IN MECHANICAL ENGINEERING
from the

NAVAL POSTGRADUATE SCHOOL
June 2002

Author: Douglas L. Williams

Approved by: Anthony J. Healey
Thesis Advisor

Terry R. McNelley,
Chairman Department of Mechanical Engineering

THIS PAGE INTENTIONALLY LEFT BLANK

ABSTRACT

In multi-vehicle mine hunting operations, it will be necessary at times for one vehicle to loiter at some point while gathering communications of data from other vehicles. The loitering behaviors of the ARIES Autonomous Underwater Vehicle have never been completely defined. The track that the vehicle chooses to maintain station while circling around one specific point for an extended period of time may be sometimes random and unpredictable, unless defined in terms of specific tracks. Simulations were run and analyzed for various conditions to record the tendencies of the vehicle during different current conditions and approach situations. The stability of the Heading Controller was then analyzed in order to predict the position where the Line of Sight Guidance algorithm becomes unstable. The data obtained through the simulations supports and explains the tendencies ARIES exhibits while circling around a loiter point.

THIS PAGE INTENTIONALLY LEFT BLANK

TABLE OF CONTENTS

ACKNOWLEDGMENTS

This work is done within the general support of funds from the Office of Naval Research. I would like to acknowledge Professor Tony Healey for his guidance, patience and motivation throughout the thesis process. His high level of technical competence and uncanny ability to teach provided me with a great understanding of the subject area. Additionally, I would like to thank LCDR John Keegan and LT Joseph Keller for their assistance and support in obtaining and interpreting data for this thesis. Finally and most importantly I would like to thank my wife, Tammy, for her love and support.

THIS PAGE INTENTIONALLY LEFT BLANK

I. INTRODUCTION

A. BACKGROUND

As Autonomous Underwater Vehicle (AUV) technology advances, mission objectives in a military environment will become more enhanced. Specifically, minefield mapping and mine reconnaissance scenarios will utilize AUVs in order to ensure personnel safety. As the possibility of military conflict continues throughout the world, the need for capable mission objectives for AUVs becomes imperative. AUVs will be involved with complex and dynamic mission assignments where data exchange between vehicles occurs frequently and objectives can change often.

A loitering technique will be introduced in a vehicle's mission capabilities to attempt to increase an AUV system objective capabilities. This will allow the vehicle to perform in a dynamic environment where data exchanges and changing mission objectives are to be completed. Loitering parameters will be introduced in the programming of the mission and will be executed upon a transition criteria being met. Such criteria are listed:

1. Receiving a command from the control station to proceed to a loiter station for data transfer or for further tasking parameters.
2. Upon mission abort from time out procedures or any other abort parameters with the exception of immediate surfacing abort criteria.
3. Upon completion of current mission assignment.

Loitering stations will be defined and introduced into the mission assignment through coding prior to the execution of the mission. There will be a specific loiter station for each leg of the AUV's defined track. If the AUV meets the criteria listed above, it will proceed to the defined loiter station for the respective leg and wait further instructions.

Before being able to test loitering missions with the AUV, modeling of the vehicle must be researched to accurately to predict vehicle characteristics during such assignments. Accurate guidance calculations become imperative in order to accomplish

the dynamic mission parameters set forth. The vehicle must reach its intended loiter point and maintain station until further instructions are received. Also, the effect of hydrodynamic forces such as waves and currents acting on the vehicle must be taken into consideration when attempting to predict the tendencies of the vehicle proceeding and maintaining position at a loiter station. If the vehicle cannot maintain station at a loitering point due to the forces acting on it then a different stationing concept must be conceived.

B. SCOPE OF THIS WORK

The loitering technique of the ARIES is not thoroughly understood. The vehicle does not maintain station at one point very well. The track that the AUV follows during a loiter maneuver is random and unpredictable. This thesis is written to break down the reasons why ARIES performs in such a way and what alternatives can be made to prevent such actions.

Chapter II will explain the general background data of ARIES. This will include current command and control configuration, hardware and software architecture, and a general explanation of the control laws that govern the vehicle's movements.

Chapter III will discuss the theory and benefits behind the implementation of loitering stations along each leg of a mine mapping mission. The parameters to transition to a loiter station will also be discussed in detail.

Chapter IV will consists of simulation data that contains various conditions that ARIES could encounter in an actual run. The simulations show the relevance of current direction acting on the vehicle and which conditions are optimal for ARIES.

Chapter V will justify the reason for the loitering behavior that the AUV exhibits when attempting to loiter around a point.

Chapter VI is a stability analysis that supports the theories that the Line of Sight Guidance is unstable when approaching the loitering point.

Chapter VII discusses options to correct for the loitering behavior and other alternatives to research in the future.

II. GENERAL BACKGROUND ON THE ARIES AUV

A. VEHICLE DESCRIPTION

(This section is largely taken from [1], but is repeated here for convenience of the reader). Construction on ARIES began in the fall of 1999 and was fully operational in the spring of 2000. The ARIES vehicle is a shallow water communications server vehicle with a Differential Global Positioning System (DGPS) and a Doppler aided Inertial Measurement Unit (IMU) / Compass navigation suite. Figure 1 shows the command and control system as it exists today.

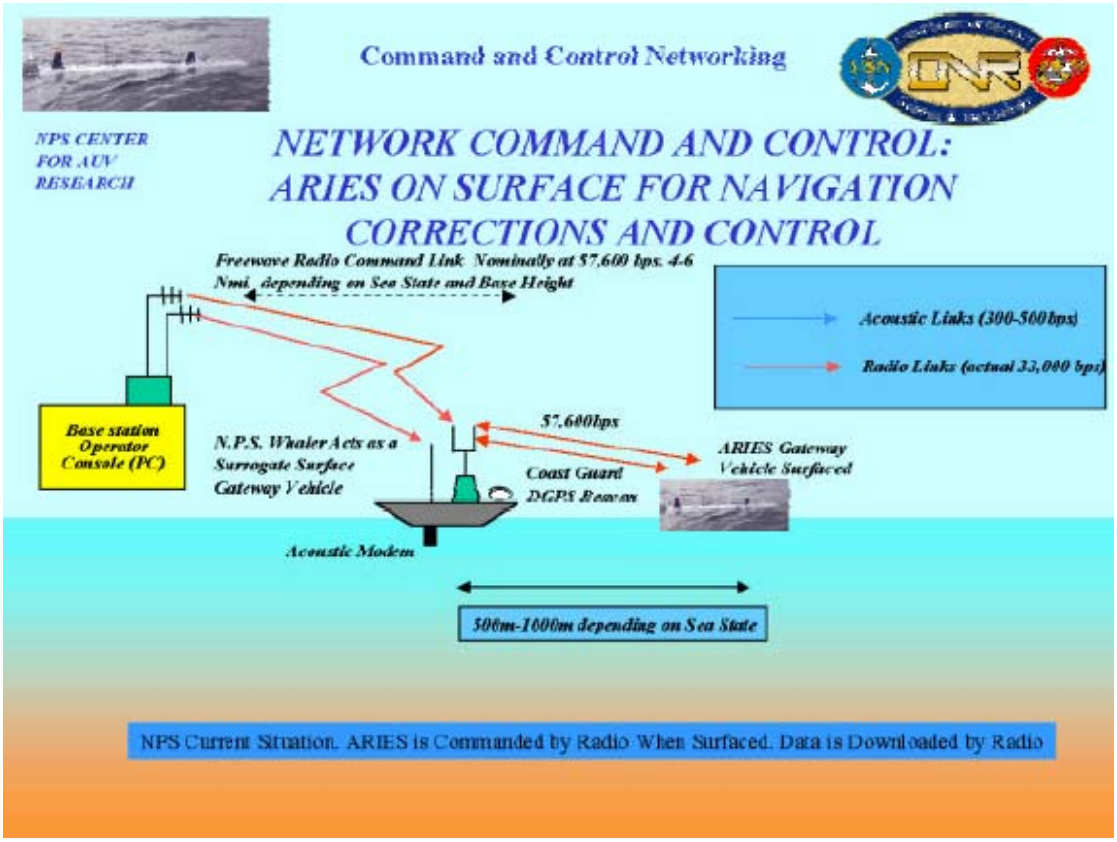

Figure 1. Current Command and Control. [1]

ARIES measures approximately 3 meters long, 0.4 meters wide, 0.25 meters high, and weighs 225 kilograms. A fiberglass nose that becomes flooded is used to house the external sensors, power switches, and status indicators. The hull is constructed of 0.25

inches thick 6061 aluminum that contains all the electronics, computers, and batteries. The ARIES is powered by six 12-volt rechargeable lead acid batteries and the endurance is approximately 3 hours at a top speed of 3.5 knots, or 20 hours hotel load only. ARIES can operate safely at a depth of 30 meters, however, through finite element analysis it has been shown through hull strengthening that ARIES can operate safely up to 100 meters. Figure 2 shows the major hardware components of the ARIES.

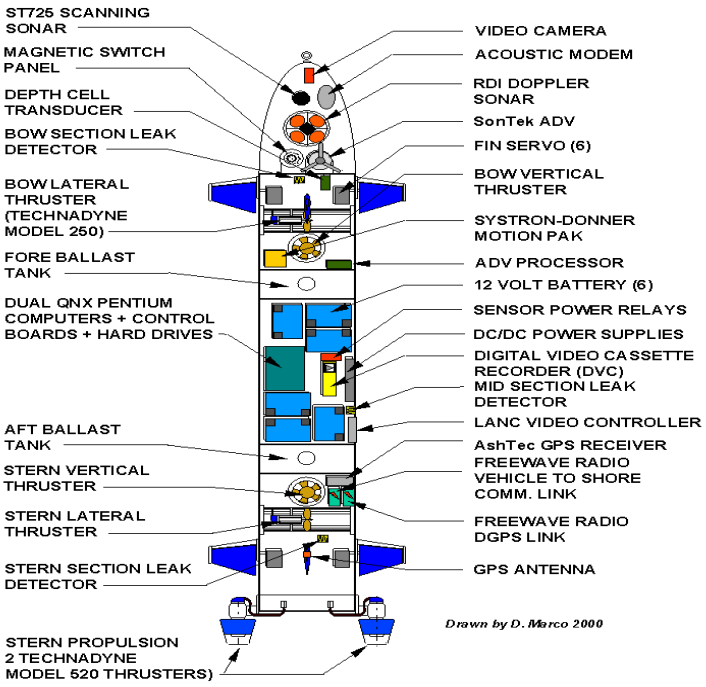

Figure 2. Hardware Components. [1]

Propulsion is achieved using twin 0.5 Hp electric drive thrusters located at the stern. Heading and depth is controlled using upper bow and stern rudders and a set of bow and stern planes, respectively. Although not currently installed on ARIES, vertical and lateral cross-body thrusters can be used to control surge, sway, heave, pitch, and yaw motions during slow or zero speed maneuvers.

The navigation sensor suite consists of a 1200 kHz RD Instruments Navigator Doppler Velocity Log (DVL) that also contains a TCM2 magnetic compass. This navigation suite measures vehicle altitude, ground speed, and magnetic heading. Angular rates and accelerations are measured using a Systron Donner 3-axis Motion Pak IMU. While surfaced, differential GPS (Ashtech G12-Sensor [2]), accuracy 40 centimeters, is available to correct any navigational errors accumulated during the submerged phases of a mission. In addition, and because of inaccuracies in the TCM2 compass, a Honeywell HMR3000 magnetic-restrictive compass, corrected by a deviation table, is used as the primary heading reference standard. Experiments have shown that the deviation table maximum error is approximately 4 degrees in some orientations.

A fixed wide-angle video camera (Deep Sea Power and Light – SS100) is located in the nose and connected to a Digital Video Cassette (DVC) recorder. The computer is interfaced to the recorder and controls the on/off and start/stop functions. The video image has the date, time, position, depth, and altitude superimposed onto it.

A scanning sonar (Tritech ST725) or a profiling sonar (ST1000) is used for obstacle avoidance and target acquisition/reacquisition. The sonar can scan continuously through 360 degrees of rotation or be swept through a defined angular sector.

Freewave Radio Modems are used for moderate bandwidth (2000-3000 bytes/sec over 4 to 6 nautical miles with repeaters) command and control (C^2), between command center and the vehicle when surfaced. Kermit file transfer protocol is used in the vehicle computer with Zmodem through Procomm protocol on the base station side. Experiments conducted have transferred data files between the surfaced ARIES, a Boston Whaler repeater station, and a base station command center. Radio modem connections require line-of-sight and are critically dependent on antennae height above ground.

ARIES has an FAU acoustic modem installed onboard, details of which are provided in [3]. The successful operation of the modem is imperative if ARIES is to be used as a network server. Other modems could be installed in the same fashion as the FAU modem allowing for more than one modem to be used during the same mission. This would allow future networking links between different vehicles without an interoperable standard in place.

B. COMPUTER HARDWARE

The dual computer system unit consists of two Ampro Little Board 166 MHz Pentium computers with 64 MB RAM, four serial ports, a network adapter, and a 2.5 GB hard drive each. Two AC/DC voltage converters for powering both computer systems and peripherals are integrated into the computer package. The entire computer system draws a nominal 48-Watts. Both systems use TCP/IP sockets over thin wire Ethernet for inter processor communications and connections to an external LAN. The sensor data gathering computer is designated QNXT, while the second is named QNXE and executes the various auto-pilots for servo level control. Both computers are used as the baseboard for a stack of Diamond Systems PC-104 data acquisition boards.

C. COMPUTER SOFTWARE

1. Architecture

Figure 3 shows a diagram outlining the modular, multi-rate, multi-process software architecture.

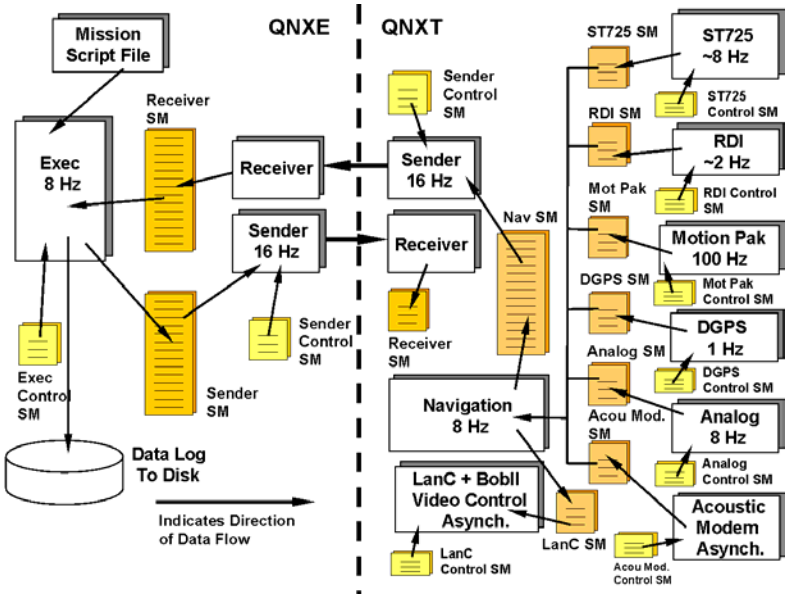

Figure 3. Dual Computer Software Architecture. [1]

This scheme is designed to operate using a single computer processor, or two independent cooperating processors linked through a network interface. Splitting the processing between two computers can significantly improve computational load balancing and software segregation. A dual computer implementation is presented here, since, in the ARIES, each processor assumes different tasks for mission operation. Both computers run the QNX real time operating system using synchronous socket sender and receiver network processes for data sharing between the two. On each processor, inter-process communication is achieved using semaphore controlled shared memory structures. Deadlocks and race conditions are explicitly eliminated by the careful use of semaphores in this system design. AT boot time, the network processes are started automatically and all shared memory segments are created in order to minimize the amount of manual setup performed by the user.

All vehicle sensors are interrogated by separate, independently controlled, concurrent processes, and there is no restriction on whether the processes operate synchronously or asynchronously. Since various sensors gather data at different rates, each process may be tailored to operate at the acquisition speed of the respective sensor. Each process may be started, stopped, or reset independently allowing easy reconfiguration of the sensor suite needed for a given mission. All processes are written in C.

To allow synchronous sensor fusion, each process contains a unique shared memory data structure that is updated at the specific rate of each sensor. All sensor data are accessible to a synchronous navigation process through shared memory and is a main feature of the software architecture. Incorporated into the navigation process is an extended Kalman filter that fuses all sensor data and computes the real time position, orientation, velocity, etc, of the vehicle. The dual compute implementation uses one processor for data gathering and running the navigation filters, while the second uses the output from the filters to operate the various auto-pilots for servo level control. Once the state information is computed, it is transmitted to the second computer over standard TCP/IP sockets.

2. Mission Control Modes

Vehicle behaviors are determined by a pre-programmed mission script file. This is parsed in the QNXE computer by the processes Exec. The file contains a sequential list of commands that the vehicle is to follow during a mission. These commands may be as simple as setting the stern propulsion thruster speeds, to more complex maneuvers such as commanding the vehicle to repeatedly fly over a submerged target at a given GPS coordinate using altitude and cross-track error control.

D. AUTO PILOT CONTROL LAWS

The ARIES uses four different auto pilots for flight maneuvering control. They consist of independent diving, steering, altitude above bottom, and cross-track error controllers. All four auto pilots are based on sliding mode control theory and each mode (i.e. diving, steering, etc) is de-coupled for ease of implementation and design. A reference for the details of controller design methodology may be found in (Healey and Lienard, 1993, [4]). The designers of the ARIES have found that Sliding Mode controllers are more simple to use and implement with minimal tuning than PID, LQR, fuzzy and heuristic control.

1. Depth Controller

Since the vehicle depth can be independently controlled by the dive planes alone, the diving controller may be modeled by a linearized system with a single generalized input control, *u(t)*, generating a pitch-dive control distributed to bow and stern planes in an equal and opposite amount, and is of the form

$$\dot{\boldsymbol{x}} = \boldsymbol{A}\boldsymbol{x} + \boldsymbol{b}u\,, \tag{1}$$

and for the ARIES, the dynamics are given by the system of equations

$$\begin{bmatrix} \dot{q}(t) \\ \dot{\theta}(t) \\ \dot{Z}(t) \end{bmatrix} = \begin{bmatrix} -1.3899 & -0.0032 & 0 \\ 1 & 0 & 0 \\ 0 & -U & 0 \end{bmatrix} \begin{bmatrix} q(t) \\ \theta(t) \\ Z(t) \end{bmatrix} + \begin{bmatrix} -2.6091 \\ 0 \\ 0 \end{bmatrix} \delta_{sp}(t) + (distur) \tag{2}$$

where, $q(t)$ is the pitch rate, $\theta(t)$ is the pitch angle, $Z(t)$ is the depth in meters, and $\delta_{sp}(t)$ is the stern plane angle in radians. U is the nominal longitudinal speed of the vehicle expressed in (m/sec) and a value of 1.8 m/sec is used. Although the bow and stern planes may be independently controlled, currently both sets of planes operate as coupled pairs such that the command to the bow planes is $-\delta_{sp}(t)$. Notice that the heave velocity, *w*, equation is ignored, as also are its effects on the *q* and *Z* equations of motion. They are considered to be disturbances. The reduction of the system to third order creates a simplification that is both valid and useful.

The sliding surface is then formed as a linear combination of state variable errors in the usual way. Ignoring any non-zero pitch angle and rate commands, the sliding surface polynomial becomes

$$\sigma(t) = 0.7693q(t) + 0.6385\theta(t) + 0.072488(Z_{com} - Z(t)) \tag{3}$$

and the corresponding control law for the stern planes is

$$\delta_{sp}(t) = 0.4994(-0.4105q(t) + 0.1086\theta(t) + \eta \tanh(\sigma(t)/\phi) \tag{4}$$

where, $\eta = 1.0$ and $\phi = 0.5$.

2. Altitude Controller

In order to control the vehicle altitude above the bottom designated $h(t)$, we simply need to change some of the signs of the terms from the diving equations. Noting the sign difference of the pitch angle and rate coefficients, this results in the following sliding surface

$$\sigma(t) = -0.7693q(t) - 0.6385\theta(t) + 0.0724(h_{com} - h(t)) \tag{5}$$

The stern plane command for altitude control is

$$\delta_{sp}(t) = -0.4994(0.4105q(t) - 0.1086\theta(t) + \eta \tanh(\sigma(t)/\phi)) \tag{6}$$

where, $\eta = 1.0$, $\phi = 0.5$, and $h(t)$ in meters replaces the vehicle depth, *Z*.

3. Heading Controller

By similar reasoning, and to eliminate the need to feedback the sideslip velocity, we argue that a second order model is sufficient. The side-slip effects are treated as disturbances that the control overcomes. Thus, the heading model becomes

$$\begin{aligned} \dot{r}(t) &= ar(t) + b\delta_r(t) + (disturbances) \\ \dot{\psi}(t) &= r(t) \end{aligned} \tag{7}$$

where, $r(t)$ is the yaw rate and $\delta_r(t)$ is the stern rudder angle. The coefficients a and b have been determined using system identification techniques from past in water experiments and are $a = -0.30\,rad/sec$ and $b = -0.1125\,rad/sec^2$. The stern and bow rudders operate in the same way as the planes, therefore, the command to the bow rudder is $-\delta_r(t)$.

Notice that in order to use this steering law, $(\psi_{com} - \psi)$ must lie between $\pm 180^0$, and is de-wrapped as needed in order to make that happen, and ignoring any non-zero command yaw rate, the sliding surface is defined by

$$\sigma(t) = -0.9499\, r(t) + 0.1701(\psi_{com} - \psi(t)) \tag{8}$$

The stern rudder command for heading control is

$$\delta_r(t) = -1.543(2.5394 r(t) + \eta \tanh(\sigma(t)/\phi)) \tag{9}$$

where, $\eta = 1.0$ and $\phi = 0.5$.

4. Cross Track Error Controller

To follow a set of straight line tracks that form the basis of many guidance requirements, a sliding mode controller is presented that has been experimentally validated under a wide variety of conditions. Other works have studied this problem for land robots, (for example, Kanayama, 1990) and usually develop a stable guidance law based on cross track error. Here, with Figure 4 as a guide to the definitions, we use a combination of a Line of Sight Guidance (Healey, Lienard, 1993) and a Cross Track Error Control for situations where the vehicle to track heading error is less than 40

degrees. For the line of sight guidance with large heading error, a separate line of sight controller is used.

One of the shortcomings of the heading controller defined above is that it has no ability to track a straight line path between two way points since it can only regulate the vehicle heading. It is desired to command the vehicle to track a line between two way points with both a minimum of error from the track and heading error between the vehicle and the track. This type of regulation is known as cross track error control and the variable definitions are illustrated in Figure 4.

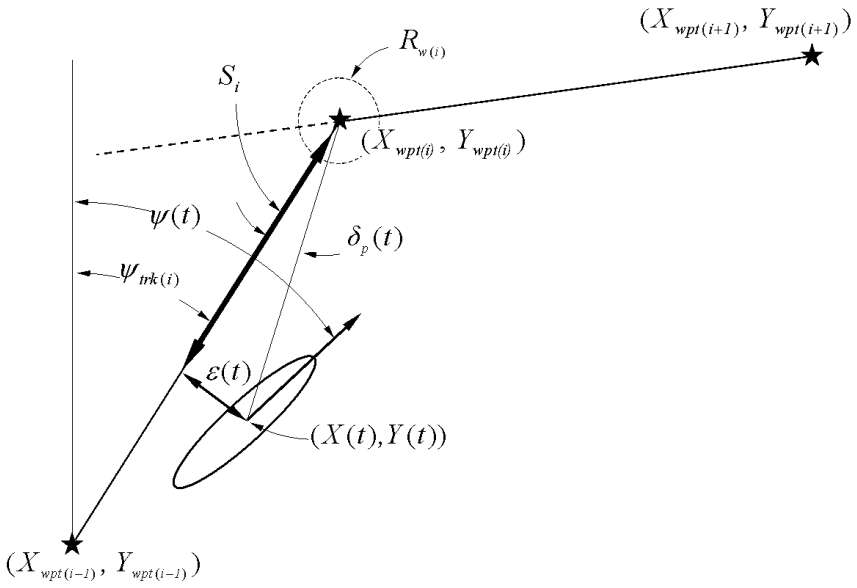

Figure 4. Cross Track Error Definitions. [1]

The variable of interest to minimize is the cross track error, $\varepsilon(t)$, and is defined as the perpendicular distance between the center of the vehicle (located at $(X(t), Y(t))$ and the adjacent track line. The total track length between way point *i* and *i-1* is given by

$$L_i = \sqrt{(X_{wpt(i)} - X_{wpt(i-1)})^2 + (Y_{wpt(i)} - Y_{wpt(i-1)})^2} \tag{10}$$

where, the ordered pairs $(X_{wpt(i)}, Y_{wpt(i)})$ and $(Y_{wpt(i-1)}, X_{wpt(i-1)})$ are the current and previous way points respectively. The track angle, $\psi_{trk(i)}$, is defined by

$$\psi_{trk(i)} \;=\; \tan^{-1}(Y_{wpt(i)} - Y_{wpt(i-1)}, X_{wpt(i)} - X_{wpt(i-1)}) \tag{11}$$

The cross track heading error $\tilde{\psi}(t)_{CTE(i)}$ for the i^{th} segment is defined as

$$\tilde{\psi}(t)_{CTE(i)} = \psi(t) - \psi_{trk(i)} \tag{12}$$

where, $\tilde{\psi}(t)_{CTE(i)}$ must be normalized to lie between $\pm 180^0$. The difference between the current vehicle position and the next way point is

$$\begin{aligned} \tilde{X}(t)_{wpt(i)} &= X_{wpt(i)} - X(t) \\ \tilde{Y}(t)_{wpt(i)} &= Y_{wpt(i)} - Y(t) \end{aligned} \tag{13}$$

With the above definitions, the distance to the i^{th} way point projected to the track line $S(t)_i$, can be calculated using

$$S(t)_i = \tilde{X}(t)_{wpt(i)}(X_{wpt(i)} - X_{wpt(i-1)}) \;+\; \tilde{Y}(t)_{wpt(i)}\,(Y_{wpt(i)} - Y_{wpt(i-1)})/L_i \tag{14}$$

therefore, $S(t)_i$ ranges from 0-100% of L_i.

The cross track error $\varepsilon(t)$ may now be defined as

$$\varepsilon(t) \;=\; S_i(t)\,sin(\delta_p(t)) \tag{15}$$

where, $\delta_p(t)$ is the angle between the line of sight to the next way point and the current track line given by

$$\begin{aligned} \delta_p(t) \;=\;& \tan^{-1}(Y_{wpt(i)} - Y_{wpt(i-1)}, X_{wpt(i)} - X_{wpt(i-1)}) \\ & - \tan^{-1}(\tilde{Y}(t)_{wpt(i)} - \tilde{X}(t)_{wpt(i)}) \end{aligned} \tag{16}$$

and must be normalized to lie between $\pm 180^0$.

With the cross track error defined, the sliding surface can be cast in terms of derivatives of the errors such that

$$\begin{aligned} \varepsilon(t) &= \varepsilon(t) \\ \dot{\varepsilon}(t) &= U\,sin(\tilde{\psi}(t)_{CTE(i)}) \\ \ddot{\varepsilon}(t) &= Ur(t)\,cos(\tilde{\psi}(t)_{CTE(i)}) \\ \dddot{\varepsilon}(t) &= \dot{Ur}(t)\,cos(\tilde{\psi}(t)_{CTE(i)}) - Ur(t)^2\,sin(\tilde{\psi}(t)_{CTE(i)}) \end{aligned}$$

The sliding surface for the cross track error controller becomes a second order polynomial of the form

$$\sigma(t) = \ddot{\varepsilon}(t) + \lambda_1 \dot{\varepsilon}(t) + \lambda_2 \varepsilon(t) \tag{17}$$

The condition for stability of the sliding mode controller is

$$\dot{\sigma}(t) = \dddot{\varepsilon}(t) + \lambda_1 \ddot{\varepsilon}(t) + \lambda_2 \dot{\varepsilon}(t) = -\eta(\sigma/\phi) \tag{18}$$

and to recover the input for control, the heading dynamics Equation (7) may be substituted into Equation (16) to obtain

$$\begin{aligned} &U(ar(t) + b\delta_r)\cos(\tilde{\psi}(t)_{CTE(i)}) - Ur(t)^2 \sin(\tilde{\psi}(t)_{CTE(i)}) + \lambda_1 Ur(t)\cos(\tilde{\psi}(t)_{CTE(i)}) \\ &+ \lambda_2 U \sin(\tilde{\psi}(t)_{CTE(i)}) \end{aligned} \tag{19}$$

Rewriting Equation (15), the sliding surface becomes

$$\sigma(t) = U r(t)\cos(\tilde{\psi}(t)_{CTE(i)}) + \lambda_1 U \sin(\tilde{\psi}(t)_{CTE(i)}) + \lambda_2 \varepsilon(t) \tag{20}$$

The rudder input can be expressed as

$$\begin{aligned} \delta_r(t) = &\left(\frac{1}{Ub\cos(\tilde{\psi}(t)_{CTE(i)})}\right)(-Uar(t)\cos(\tilde{\psi}(t)_{CTE(i)}) \\ &+ U(r(t))^2 \sin(\tilde{\psi}(t)_{CTE(i)}) - \lambda_1 Ur(t)\cos(\tilde{\psi}(t)_{CTE(i)}) \\ &- \lambda_2 U \sin(\tilde{\psi}(t)_{CTE(i)}) - \eta(\sigma(t)/\phi)) \end{aligned} \tag{21}$$

where, $\lambda_1 = 0.6$, $\lambda_2 = 0.1$, $\eta = 0.1$, and $\phi = 0.5$. To avoid division by zero, in the rare case where $\cos(\tilde{\psi}(t)_{CTE}) = 0.0$ (i.e. the vehicle heading is perpendicular to the track line) the rudder command is set to zero since this condition is transient in nature.

5. Line of Sight Controller

When the condition arises that the magnitude of the cross track heading error $\left|\tilde{\psi}(t)_{CTE(i)}\right|$ exceeds 40^0, a Line of Sight Control (LOS) is used. In this situation, the heading command can be determined from

$$\psi(t)_{com(LOS)} = \tan^{-1}(\tilde{Y}(t)_{wpt(i)}, \tilde{X}(t)_{wpt(i)}) \tag{22}$$

and the LOS error from

$$\tilde{\psi}(t)_{LOS} = \psi(t)_{com(LOS)} - \psi(t) \tag{23}$$

and the control laws used for heading control, Equations (8,9) may be used.

Two conditions may be true for the waypoint index to be incremented. The first and most usual case is if the vehicle has penetrated the way point watch radius $R_{w(i)}$. Secondly, if a large amount of cross track error is present, the next way point will become active if the projected distance to the way point $S(t)_i$ reached some minimum value $S_{min(i)}$, such that

$$if \left(\sqrt{(\tilde{X}(t)_{wpt(i)})^2 + (\tilde{Y}(t)_{wpt(i)})^2} \leq R_{w(i)} \;||\; S(t)_i < S_{min(i)} \right) \quad \text{THEN}$$

Activate Next Way Point

In water experimental results using the controllers presented above will now be presented in the next section.

E. NAVIGATION

The ARIES vehicle uses an INS / DOPPLER / DGPS navigational suite and an Extended Kalman Filter (EKF) which was developed and presented in ([5] and [6]), and may be tuned for optimal performance given a set of data. The main impediments to navigational accuracy are the heading reference and the speed over ground measurement. In this system, the heading reference is derived from both the Honeywell compass and the Systron Donner IMU, which provides yaw rate. The fusion of the yaw rate and the compass data leads to an identification of the yaw rate bias, which is assumed to be a constant value. The compass bias, which is mostly dependent on vehicle heading relative to magnetic north, is identified in the EKF ([6]), using DGPS positions when surfaced. When submerged, the position error covariance grows, but is corrected on surfacing. A relatively short surface time, (for example, 10 seconds) allows the filter to re-estimate biases, correct position estimates and continue with improved accuracy. As a demonstration, the ARIES vehicle was operated in Monterey Bay, in a series of runs

including a dive-surface-dive-surface sequence. Figure 5, below shows a plot of vehicle position in an exercise where the vehicle is commanded to follow a track at depth, come up for a DGPS correction, then follow the bottom at an altitude of 3m, while a video is recorded from a down-looking camera. The vehicle then surfaces to get a second fix before turning round and repeating the exercise from the complementary heading. In this plot, the vehicle trajectory is designed to fly over the Monterey Inner Shelf Observatory (MISO) Instrument Frame placed in 12 meters of water approximately 0.5 kilometers from shore with estimated GPS position used to design the approach lane. The video taken as the vehicle flies over the MISO is designed to provide identification details of the arbitrary object given its approximate DGPS location point.

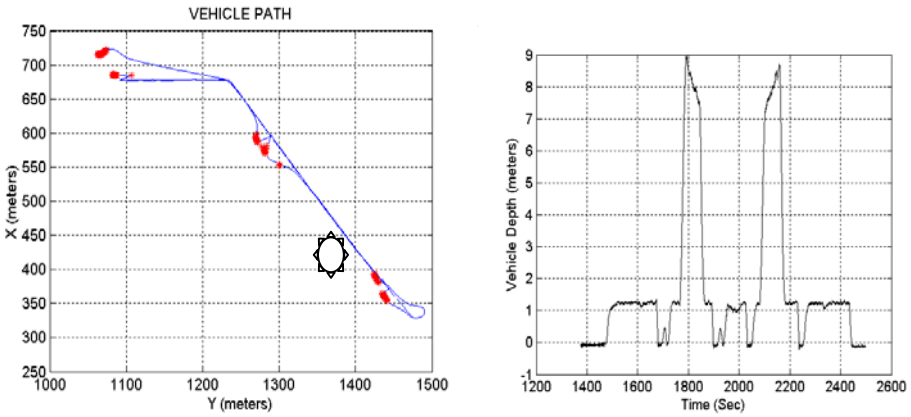

Figure 5a. Vehicle Path showing locations where the GPS position fixes were obtained by surfacing for 20 seconds (asterisks). Figure 5b. Depth Response during run that clearly shows the DGPS pop up maneuvers. [1]

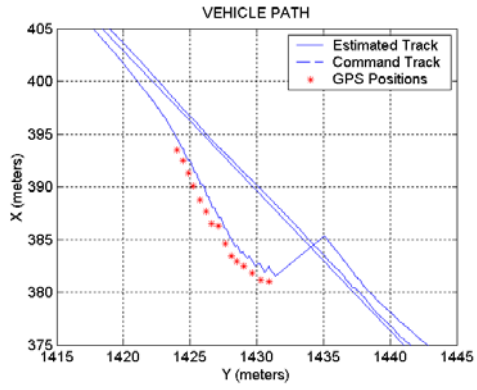

Figure 6. Close up of the final surface showing the filter solution together with the DGPS measurement at the surface. [1]

In Figure 6, a close up of the final surfacing maneuver shows that there is great consistency in estimating the true DGPS data point as seen by the AshTec G-12 unit on board. The difference between the Kalman Filter solution and the DGPS data points while surfaced is sub meter precision. However, the difference between the dead reckoning solution underwater is a few meters off the mark.

In Figure 7, the number of visible satellite vehicles seen by the DGPS unit are shown to evolve quickly. Within 10 seconds, 9 satellites are being used to compute the position solution.

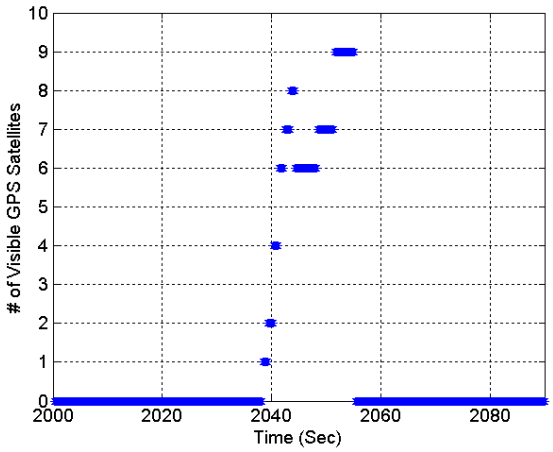

Figure 7. Time History of the response of the number of visible GPS satellites during the surface phase shown in Figure 6. [1]

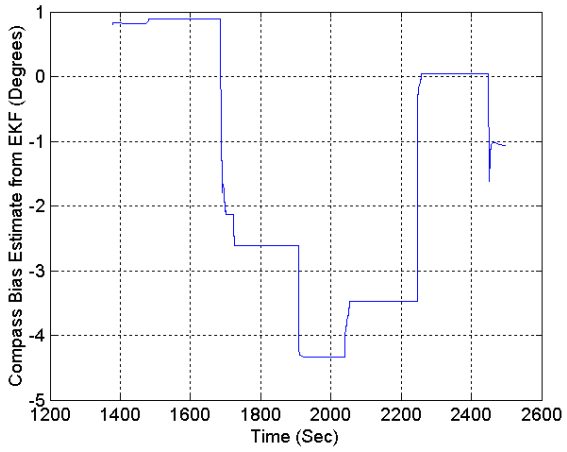

Figure 8. Compass Bias Estimate versus Time. [1]

Figure 8 shows the response of the heading bias estimate from the EKF for the entire run. At each surface approximately 10 DGPS points are obtained which rapidly corrects the compass bias. However, as is seen, compass corrections in the neighborhood of 5 degrees are still needed to predict correctly the vehicle positions. This is an indication that further corrections of the compass deviation table are needed. The remaining question is whether or not the deviations are predictable or random. While some additional runs suggest that there may be some degree of consistency, it remains to be shown conclusively.

THIS PAGE INTENTIONALLY LEFT BLANK

III. LOITERING PARAMETERS AND IMPLEMENTATION

A. GENERAL THEORY

As discussed earlier, a series of parameters must be met before the ARIES can transition to a loiter point. Figure 9 gives a graphic description of the transitions that must occur.

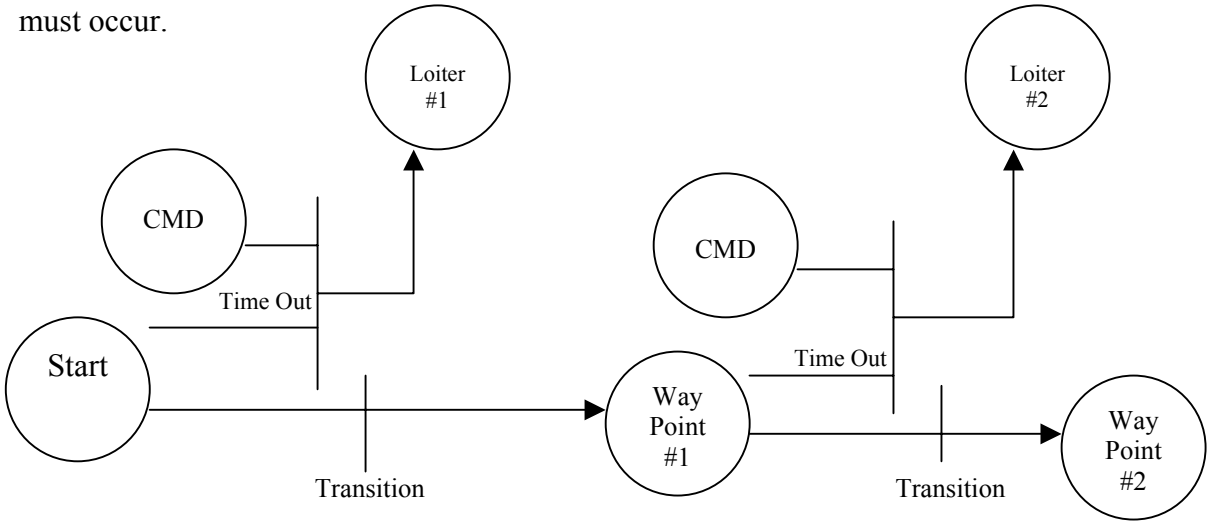

Figure 9. Loiter Logic. [7]

If the ARIES "times out" prior to reaching the next waypoint, meaning the AUV does not reach the next waypoint in the allotted amount of time, or if the vehicle receives a command (CMD) from the controlling station, the vehicle will proceed to the respective loiter point, depending on the leg that ARIES is on. Normally the AUV aborts its mission completely if there is "time out" prior to reaching the next intended waypoint. Having the vehicle proceed to a loiter point instead of aborting the entire mission allows the vehicle to maintain station at the loiter point and receive new mission parameters and/or commands from the control station instead of aborting the entire mission all together. If the criteria set forth for transition to the next waypoint is met, the vehicle will proceed as programmed until commanded by the control station to proceed to a loiter point. This logic allows flexibility for the vehicle to continue on its mission until the control station requires it to break off its pre-programmed track because of possible rendezvous with another vehicle for data transfer or adjusting mission parameters.

B. LOITER POINT MAPPING

Generally, for a given mine mapping mission, the vehicle will have a series of tracks to follow in sequence termed "legs". Figure 10 below is a typical diagram of the legs ARIES would follow for a mine mapping mission.

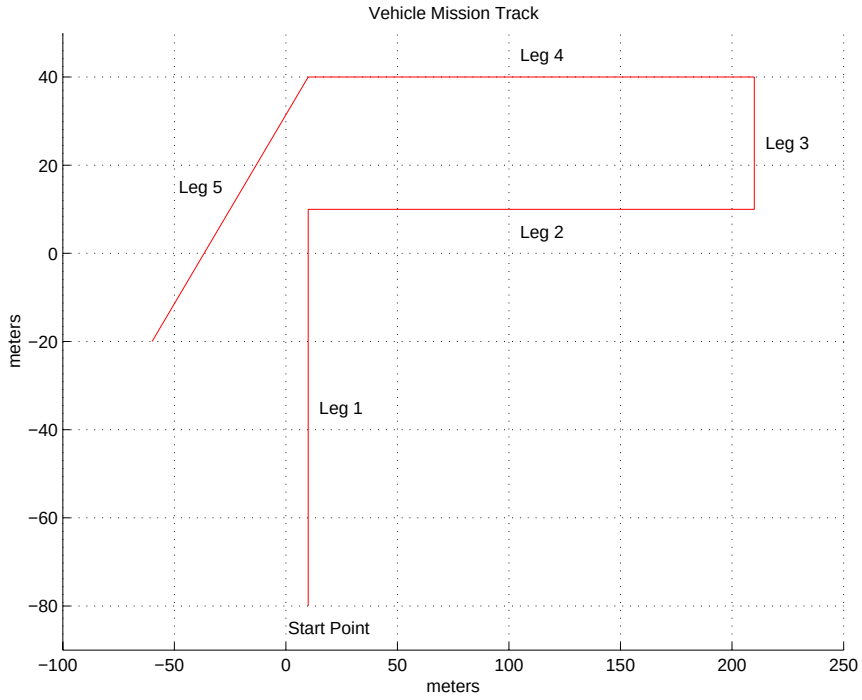

Figure 10. Typical Legs for a Mine Mapping Mission.

The idea for implementing loitering with the ARIES is to have pre-programmed loiter points within the program itself. More specifically, each leg would have a specific loiter point designated to it. As the ARIES travels down each leg, there is a respective loiter point attached to the leg. Figure 11 gives a graphical description of the loiter points and their respective legs. Note that the position of the loiter points are arbitrary and should be determined by the programmer according to the mission objectives and parameters.

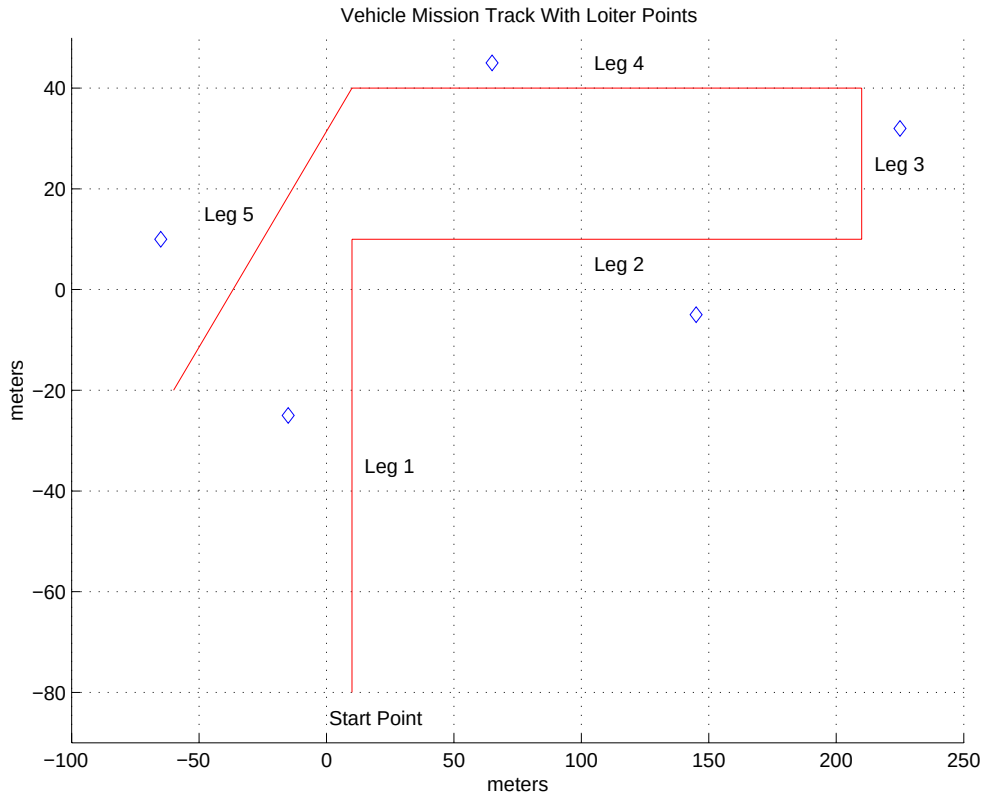

Figure 11. Loiter Points and their Respective Legs.

Positioning the loiter points in this manner allows the vehicle to transition to a loitering point and receive further instructions in the shortest amount of time. As the AUV transitions to the next leg, the previous loiter point is dropped and the new loiter point is picked up with the current leg. As the vehicle transitions to each leg, each loiter point is automatically transitioned with its respective waypoint. This reduces confusion for the control station when concentrating on command and control.

THIS PAGE INTENTIONALLY LEFT BLANK

IV. LOITERING SIMULATIONS

A. MATLAB SIMULATIONS WITH NO CURRENT

A MATLAB program was modified to include a loiter point on the first leg of the track. At an arbitrary time along the first leg, the operator is given a choice to proceed to Loiter Point 1 or continue on track. Under real operating conditions the AUV would be interrupted during its mission and commanded to a respective loiter point. However, since MATLAB is not a real time operating program the program itself had to be interrupted to interpret the operator's intentions. Below is a figure that shows what was explained above.

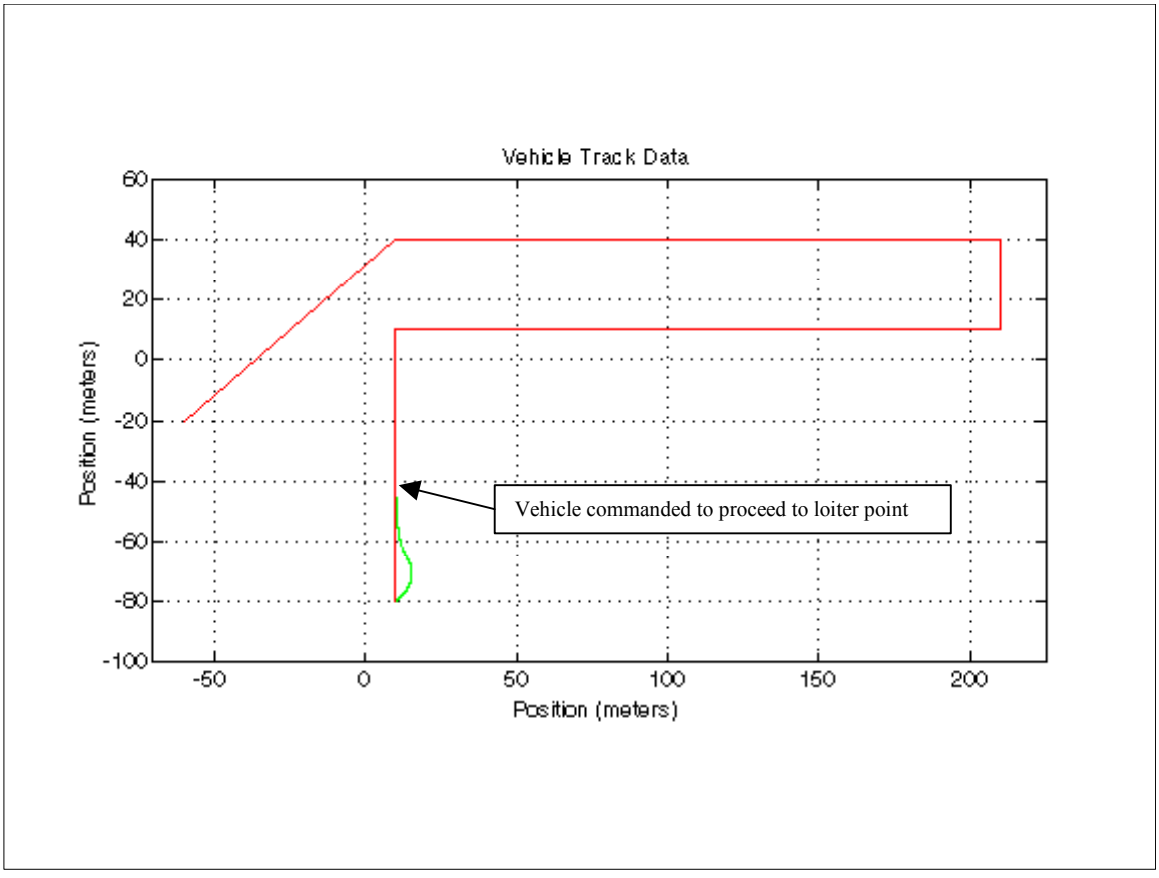

Figure 12. Arbitrary Position Along Track AUV is Ordered to Loiter Point.

The simulation has an input break built into the program to find the operator's intentions. At this point the operator either chooses to continue on track or to proceed to

a loiter point. The next figure shows the vehicle as it is commanded to proceed to a loiter point.

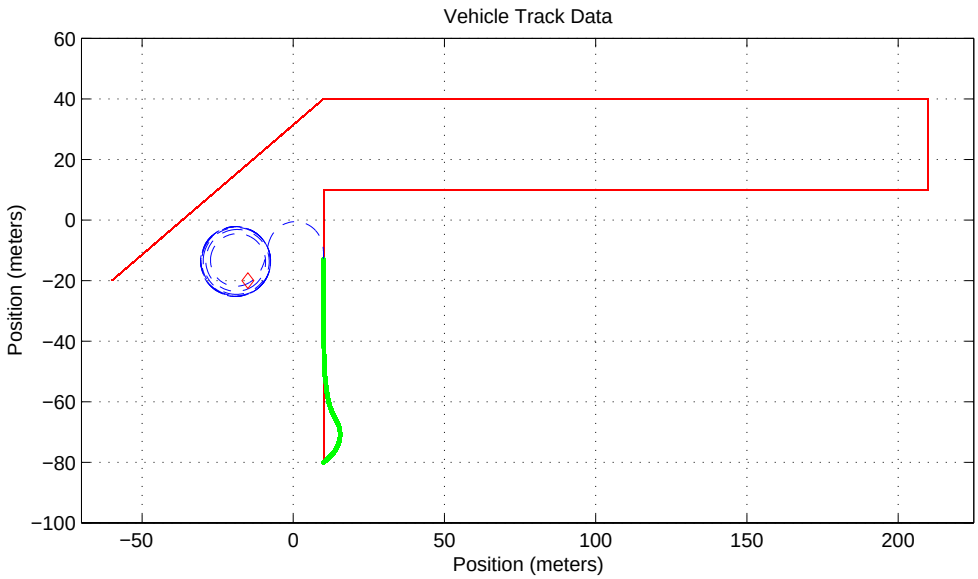

Figure 13. Vehicle Characteristics During a Loiter of 62 seconds.

Once the vehicle is commanded to proceed to the loiter point, it uses its normal Line of Sight and Cross Track Error guidance to proceed to the loiter point. The watch radius around the loiter point is set to zero so that the ARIES "never reaches" the point and thus, continues to circle or loiter. Figure 13 shows that ARIES maintains a tight bounded circular shape around the point of approximately 20 meters in diameter. As the AUV continues to loiter it should report its GPS position every 10 – 15 minutes to the control station in order to update the operators and correct itself for position errors. As ARIES is in the loiter, the control station can determine what and if mission parameters need to be changed such as, rendezvous with another vehicle, change the current track, or continue on the original track.

Figure 14 is a simulation that shows the vehicle as it continues from its loiter point back to the original track.

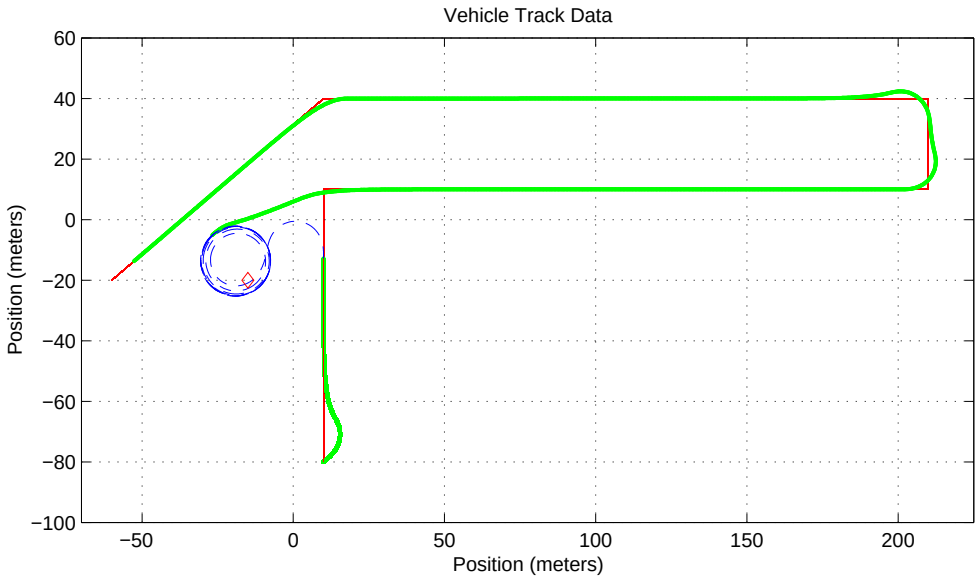

Figure 14. Continue onto Original Track From Loiter Point

Figure 14 shows how the ARIES can continue from its loiter point to its original track. ARIES has no problem transitioning from a loiter mission to resuming its previously programmed search mission.

B. MATLAB SIMULATIONS WITH CURRENT

1. Current Condition Simulation #1

The results of the simulations change drastically when a current is introduced. For condition #1, a current of 0.3 kts at a direction of 135 degrees (Southeast) is introduced in the program. The vehicle continues to operate correctly as it travels down its pre-programmed search track and proceeds to the loiter point, but when it attempts to loiter around the designated point the vehicle no longer maintains a tight, circular shape. Figure 15 shows the pattern that ARIES follows when current is introduced into the simulation.

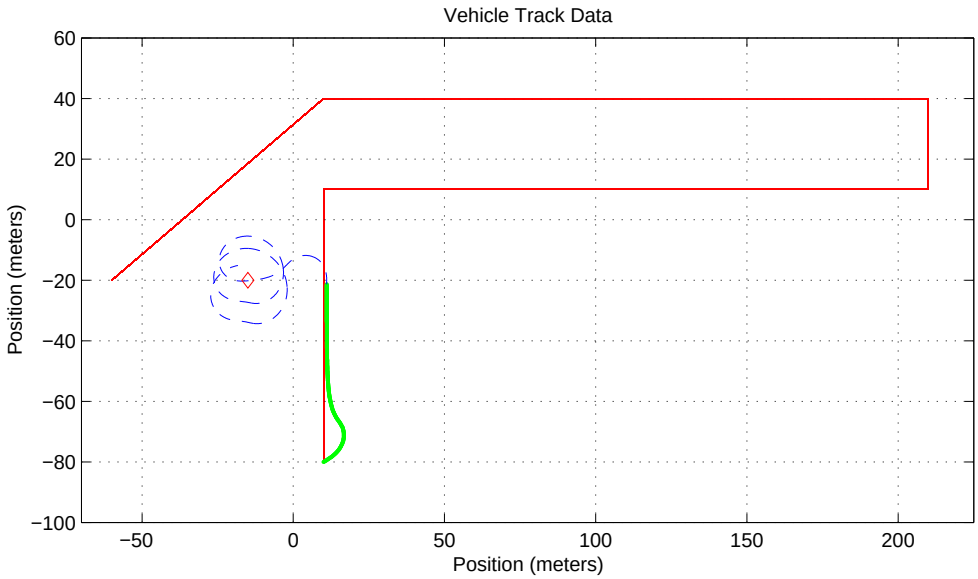

Figure 15. Loitering Track with Current for 25 seconds.

The parameters for the Figure 15 simulation has the vehicle proceeding to the loiter point by making a heading change of approximately 90 degrees. The vehicle circles around the loiter point for approximately 25 seconds. The current causes the ARIES AUV to fall off its tight, circular pattern that we viewed in Figures 13 and 14. The pattern is still somewhat circular in nature, but as ARIES continues to attempt to drive over the loiter point, the vehicle's track is slowly shifting to the south. Figure 16 is a closer view of the vehicle's track around the loiter point.

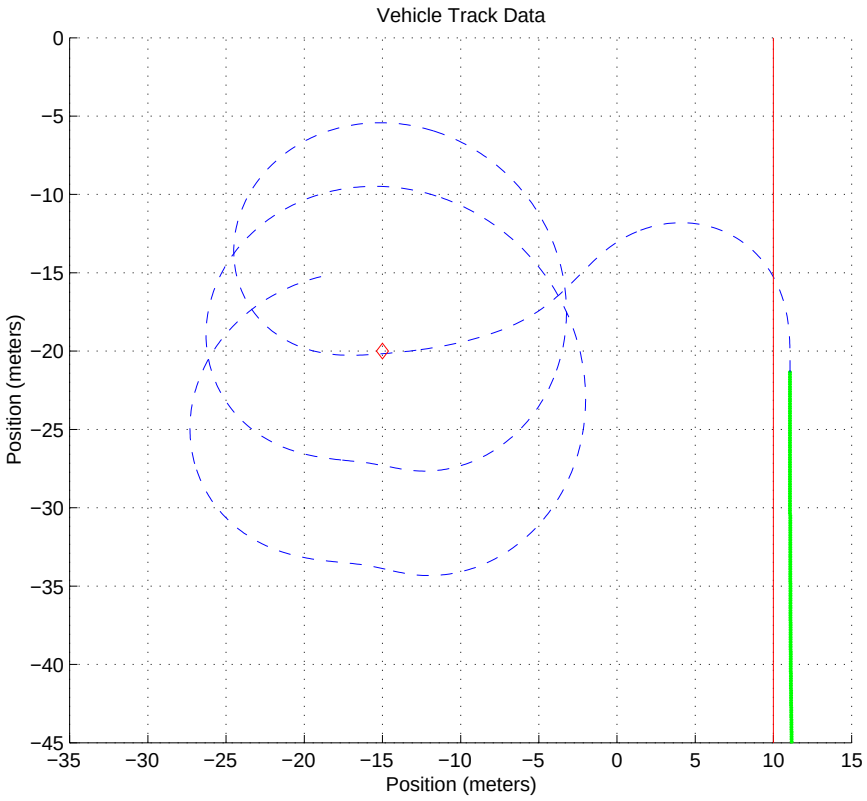

Figure 16. Close Up View of Vehicle Loiter Track After 25 Seconds with Current.

From Figure 16, it is observed that the vehicle proceeds to the loiter point as commanded. Once it passes over the point it continues to circle because the loiter point has a radius of zero, therefore, the vehicle never reaches the "waypoint" and continues to try until it does. The set and drift of the current acts on the vehicle and the tight circular shape that ARIES exhibited with no current is shifted in a southerly direction.

Figure 17a shows the vehicle track after 32 seconds. ARIES continues its circular pattern with a series of right turns until it is too far south of the loiter point and shifts the rudder. Now a circular pattern with a series of left turns exists. Figure 17b shows the AUV at 35 seconds as it is in a series of left turns in its attempt to pass over the loiter point.

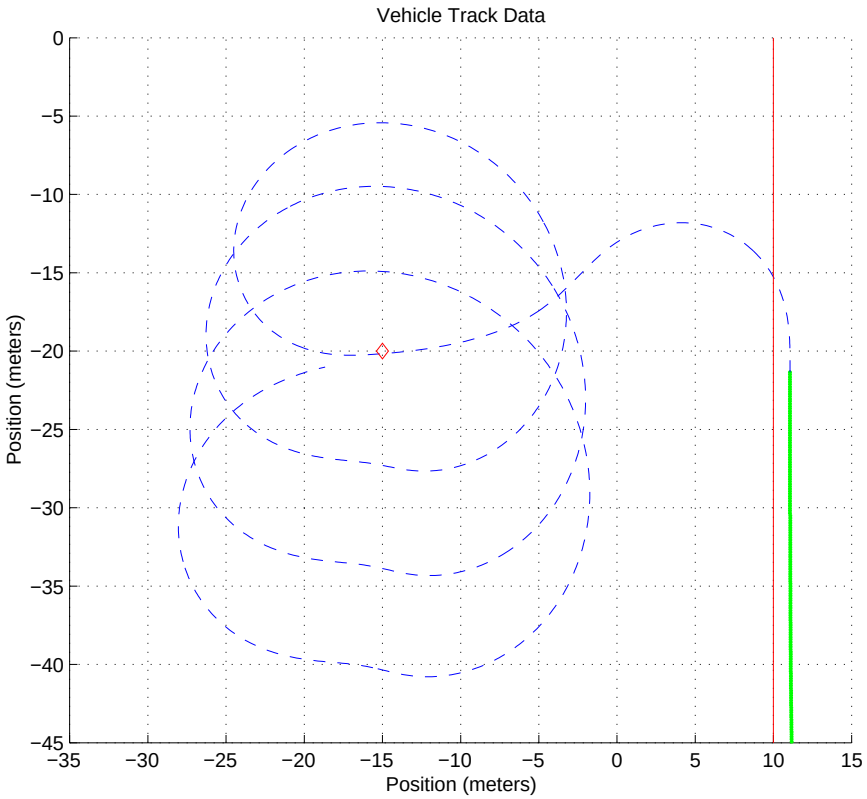

Figure 17a. ARIES is south of the loiter point and begins to make a left turn after 32 seconds.

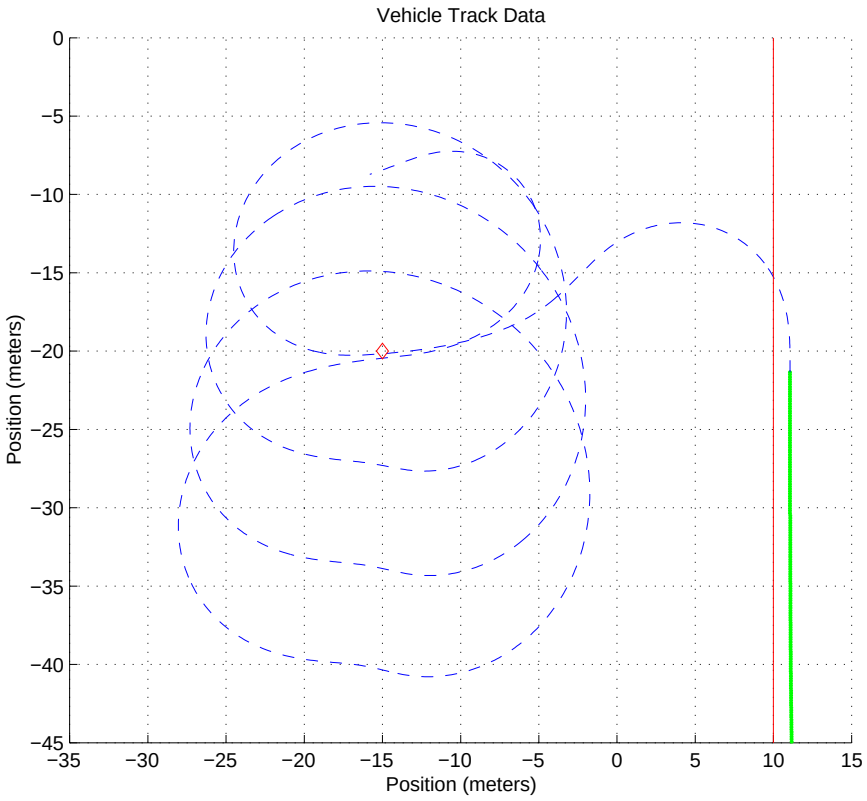

Figure 17b. ARIES in a Left Turn after 35 seconds.

Figures 17a and 17b begin to explain the "figure 8" tendencies that the AUV exhibits when loitering around one specific point. During prior missions in open waters, ARIES would not maintain a tight circular shape, rather, it would conduct a series of "figure 8" maneuvers while maintaining station around a loiter point. Figure 18 below shows the rudder angle of ARIES as it travels along its original track and then when commanded to loiter.

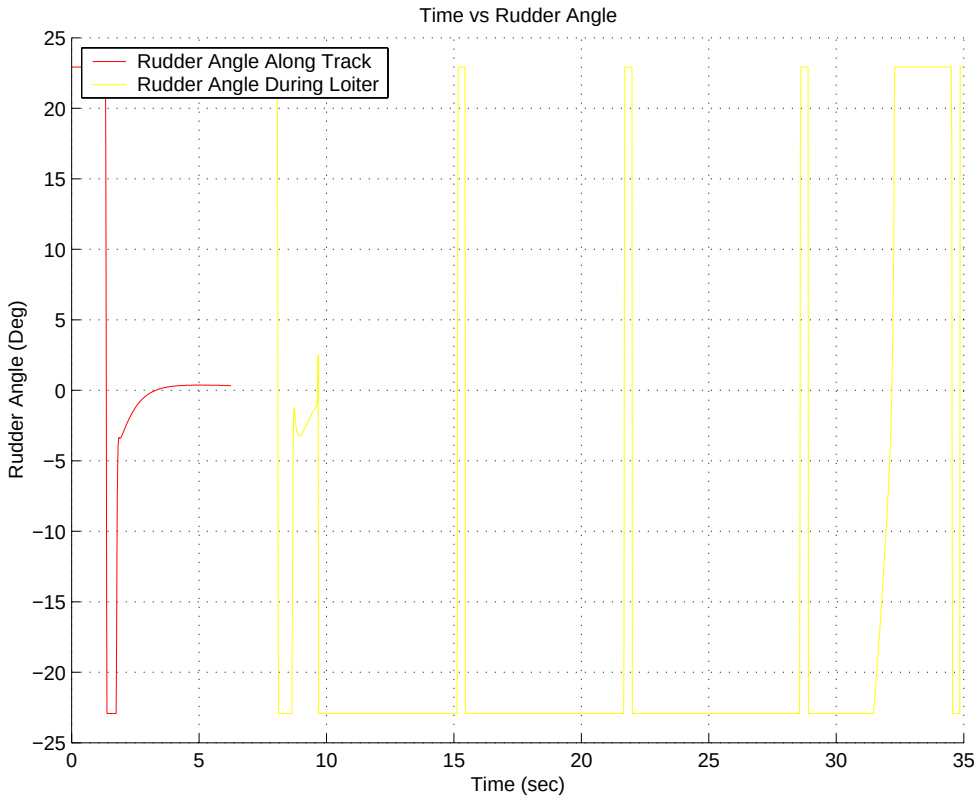

Figure 18. Rudder Angle of ARIES During Original and Loiter Track.

Figure 18 shows the rudder angle during the right and left turns as ARIES circles around the loiter point. At approximately 30 seconds the vehicle changes from right turns to left turns.

The reason why ARIES knows to change from right turns to left turns lies within Equation (16) where, $\delta_p(t)$ is the angle between the line of sight to the next waypoint and the current track line given by

$$\begin{aligned} \delta_p(t) \;=\; & \tan^{-1}(Y_{wpt(i)} - Y_{wpt(i-1)}, X_{wpt(i)} - X_{wpt(i-1)}) \\ & - \tan^{-1}(\widetilde{Y}(t)_{wpt(i)} - \widetilde{X}(t)_{wpt(i)}) \end{aligned} \tag{16}$$

and must be normalized to lie between $\pm 180^0$. Normalizing $\delta_p(t)$ allows the vehicle to pick the shortest route to the waypoint. In other words, instead of having the vehicle turn 270 degrees to starboard to reach the waypoint, it only turns 90 degrees to port.

As the loitering time is increased, the ARIES continues to exhibit the "figure 8" track description for its loitering technique. As the current sets the vehicle in different positions, the AUV properly determines the shortest route to reach the loitering point. Figure 19 shows the vehicle loitering track at 50 seconds. It is hard to tell, but as the vehicle is in a port turn, it begins to pass the loitering point on the south side, with the loiter point on the starboard beam. It computes that the shortest way to the point is to starboard and makes the correct decision by turning right.

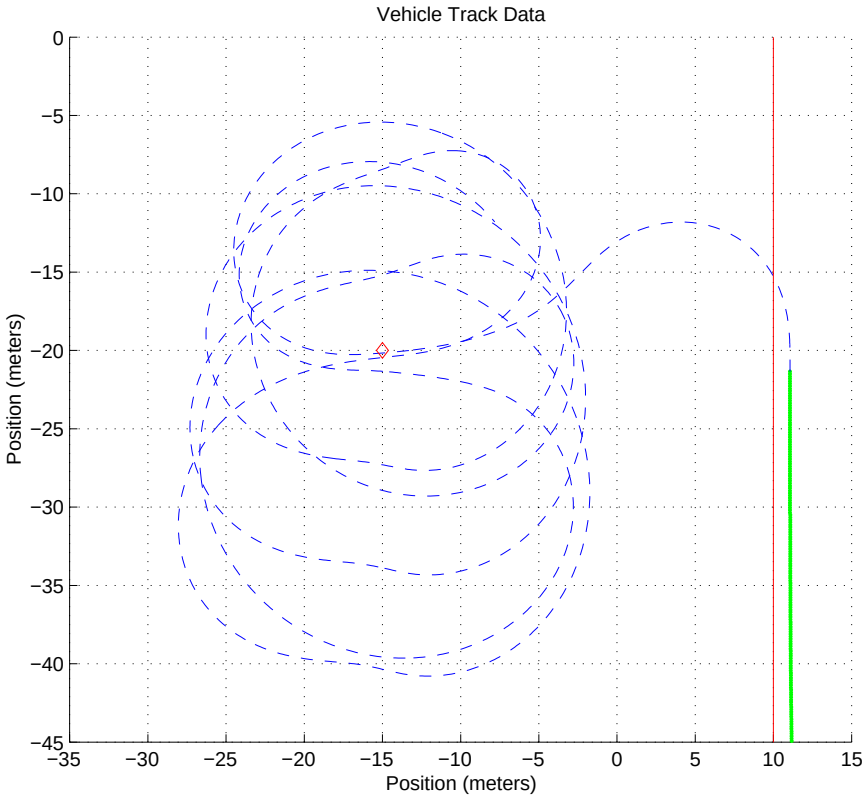

Figure 19. Loitering Track after 50 seconds.

Next, Figure 20 shows the rudder angle changing from a port turn to a starboard turn at approximately 45 seconds.

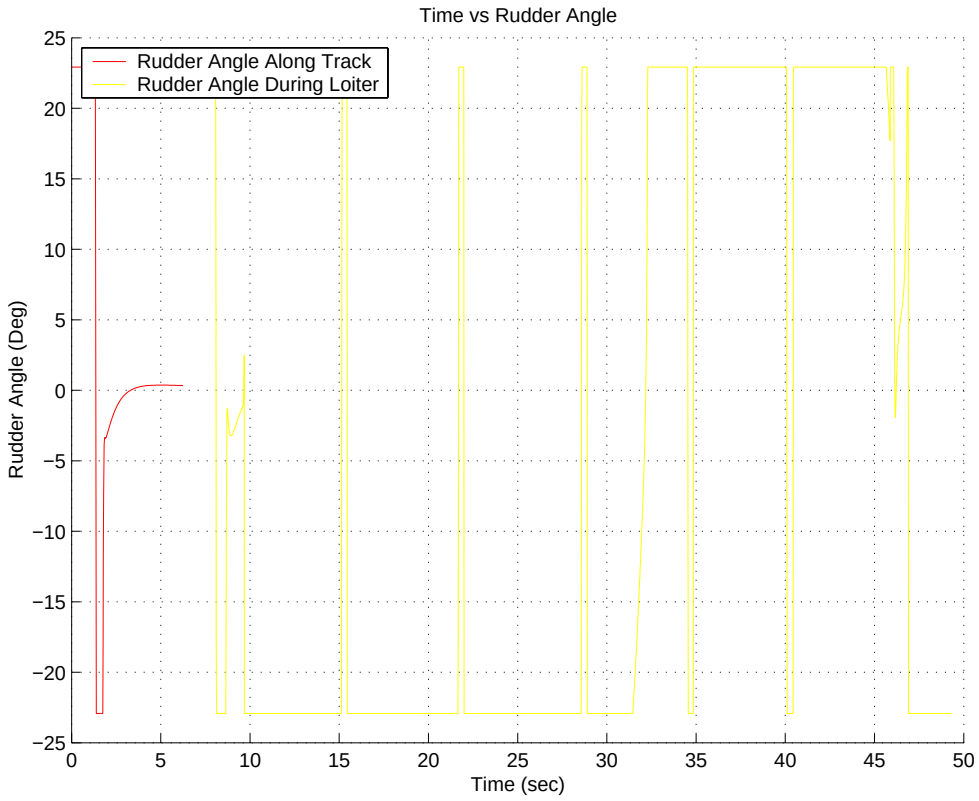

Figure 20. Time vs Rudder Angle.

2. Current Condition Simulation #2

The loitering initiation position was adjusted and the results were very interesting. The point at which the vehicle transitioned to its loiter point was changed to the beginning of its original track so that it would proceed to its loiter point by traveling directly against the current. The loitering time was kept at 50 seconds. The results are below in Figures 21, 22, and 23. The vehicle has no trouble maintaining a relatively tight, circular bounded shape around the loiter point. ARIES maintains station around the loiter point with a continuous port turn with slight adjustments during station keeping.

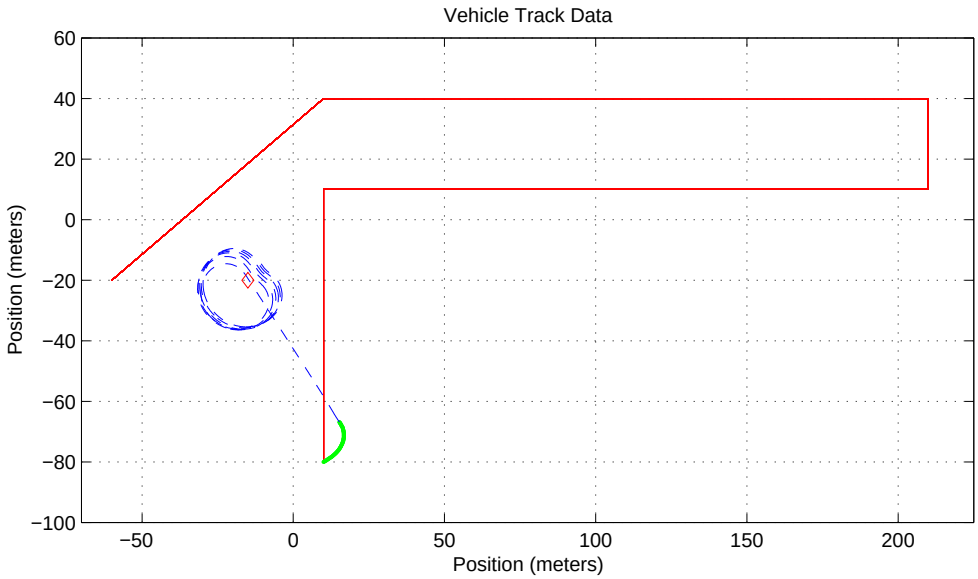

Figure 21. Loitering track after 50 seconds with vehicle proceeding into the SE setting current as it travels to the loiter point.

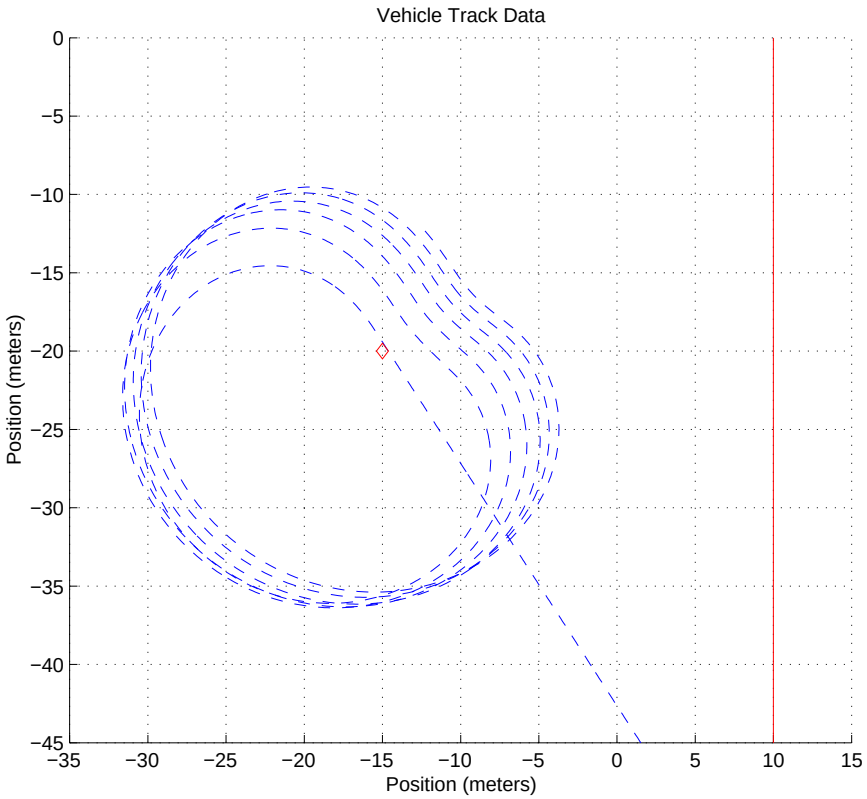

Figure 22. Loitering track after 50 seconds with vehicle proceeding into the SE setting current as it travels to the loiter point.

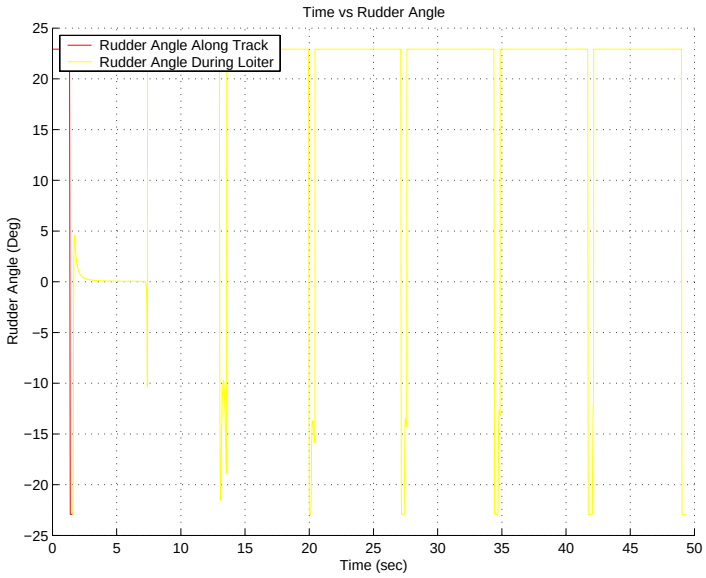

Figure 23. Time vs Rudder Angle.

The vehicle is able to maintain station on the loiter point much better as it proceeds into the onsetting current prior to loitering. Figure 24 below is the vehicle after loitering 125 seconds.

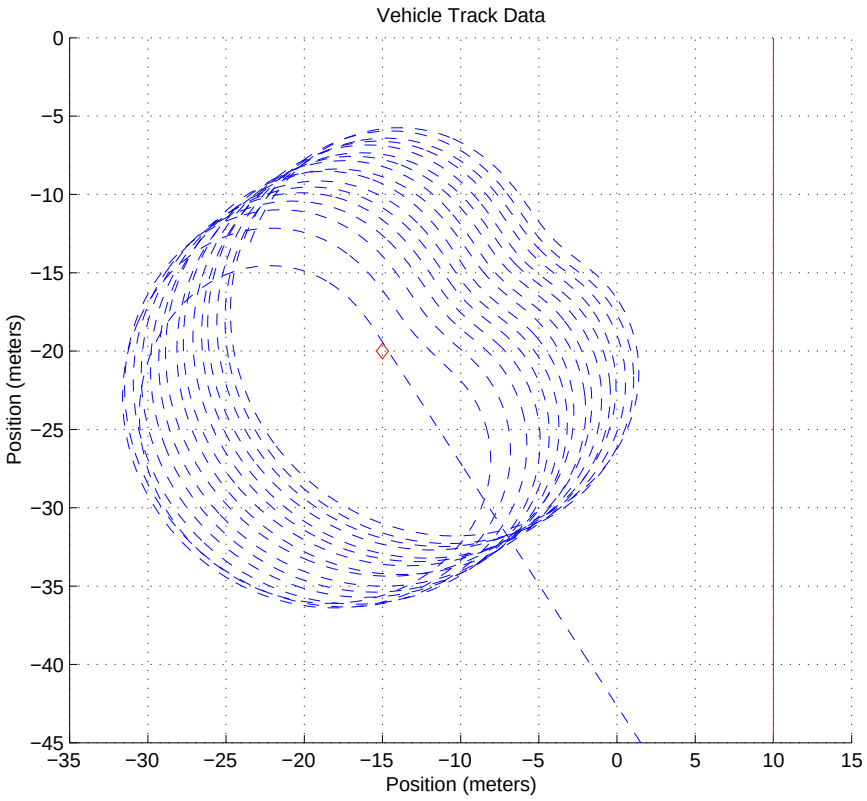

Figure 24. Loitering Track after 125 seconds.

The vehicle is slowly shifting its loitering track towards the northeast, but it is much more regular in shape as time transpires than the previous condition.

There appears to be a relationship with the approach to the loiter point and the direction of the current.

3. Current Condition Simulation #3

A simulation to establish a relationship between the loiter point approach and direction of the current was run. The direction of the current was changed to a Northeasterly direction of approximately 045 deg T and the approach to the loiter point was made later in the original track run so the vehicle would be traveling directly against the current again. Figures 25, 26, and 27 are the results of the test.

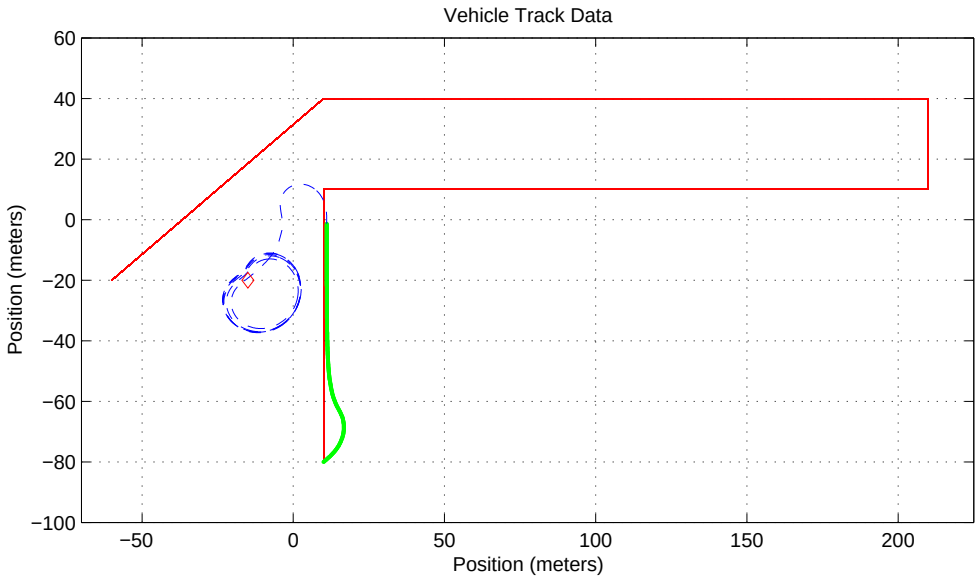

Figure 25. Loitering track after 50 seconds with vehicle proceeding into the NE setting current as it travels to the loiter point.

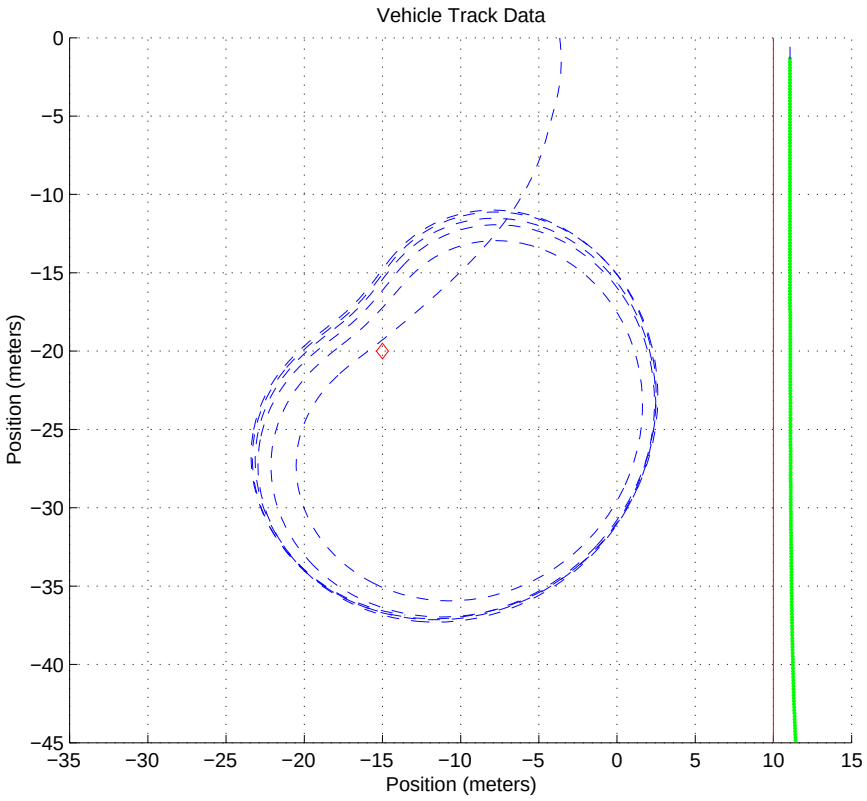

Figure 26. Loitering track after 50 seconds with the vehicle proceeding into the NE setting current as it travels to the loiter point.

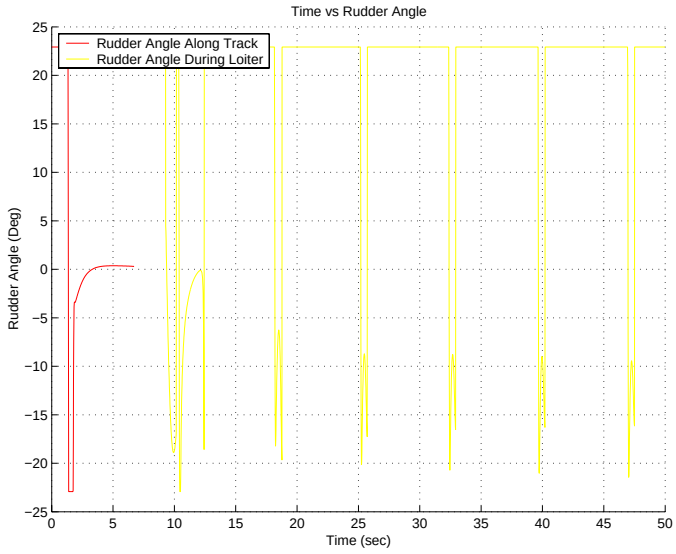

Figure 27. Time vs Rudder Angle.

From analyzing Figures 21-27, there appears to be a relationship between the loitering technique of the vehicle and the approach of the AUV to the loiter point as it relates to the direction of the current.

4. Current Condition Simulation #4

A simulation with a current traveling with the vehicle to the loiter point is created in Figures 28, 29, and 30. The ARIES exhibits the "figure 8" loitering technique in this current scenario. Current is 0.3 kts in a Northwesterly direction of approximately 315 deg T with the approach to the loiter point being at the beginning of the mission track. The loitering simulation time is kept at 25 seconds because the loitering track gets too hard to distinguish.

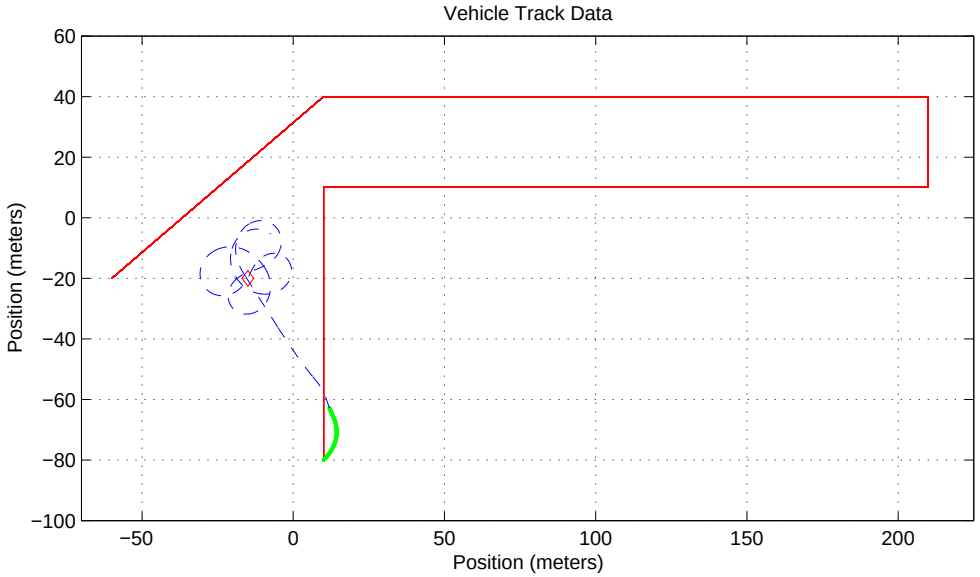

Figure 28. Loitering Track after 25 seconds with a NW setting current.

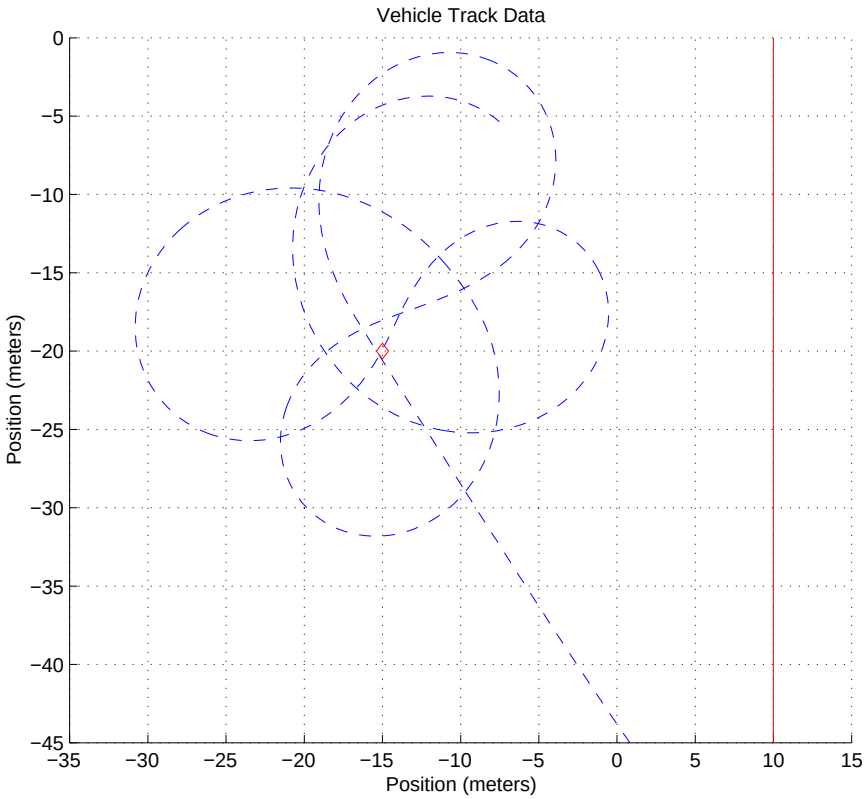

Figure 29. Loitering Track after 25 Seconds with a NW Setting Current.

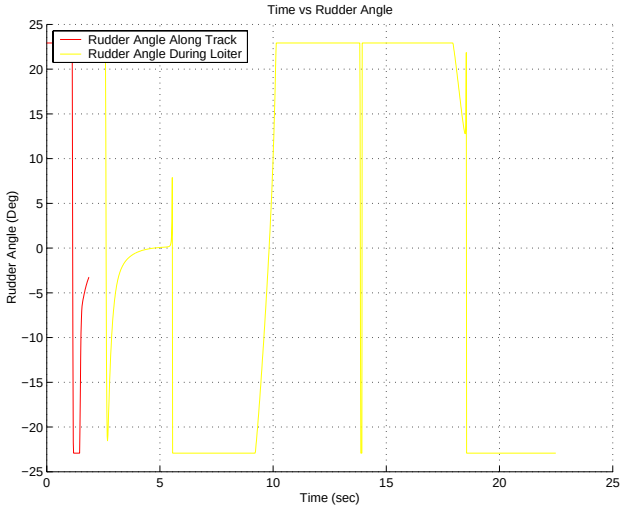

Figure 30. Time vs Rudder Angle.

After analyzing the Figures 28-30, the shape of the loiter track at every turn with this current condition is in a “figure 8”.

5. Current Condition Simulation #5

The current speed was increased to 1 kt for the same situations in the simulations run earlier (Figures 15-30). Figures 31 and 32 below shows how the vehicle loitering characteristics change with an increase in the current speed.

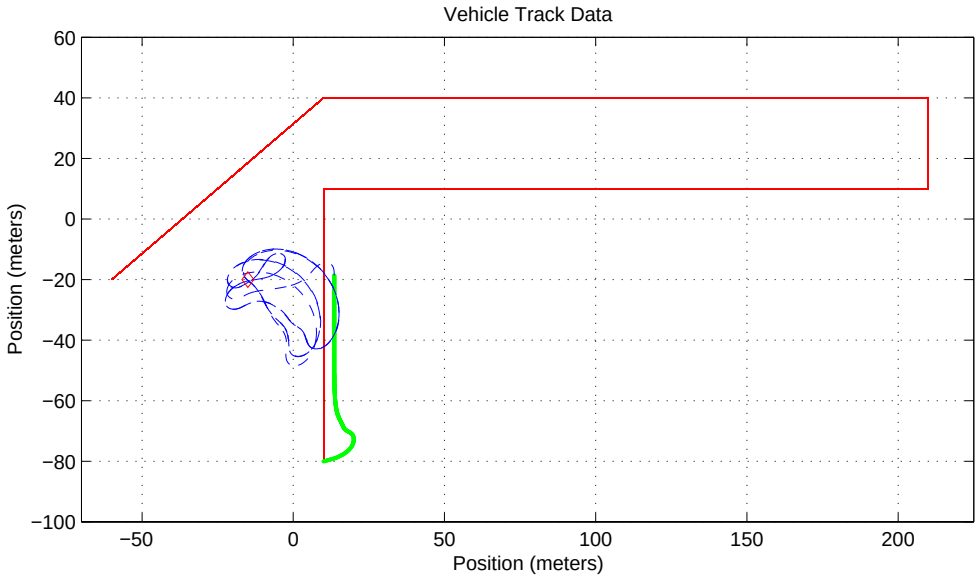

Figure 31. Loitering Track after 90 Seconds with a SE Setting Current.

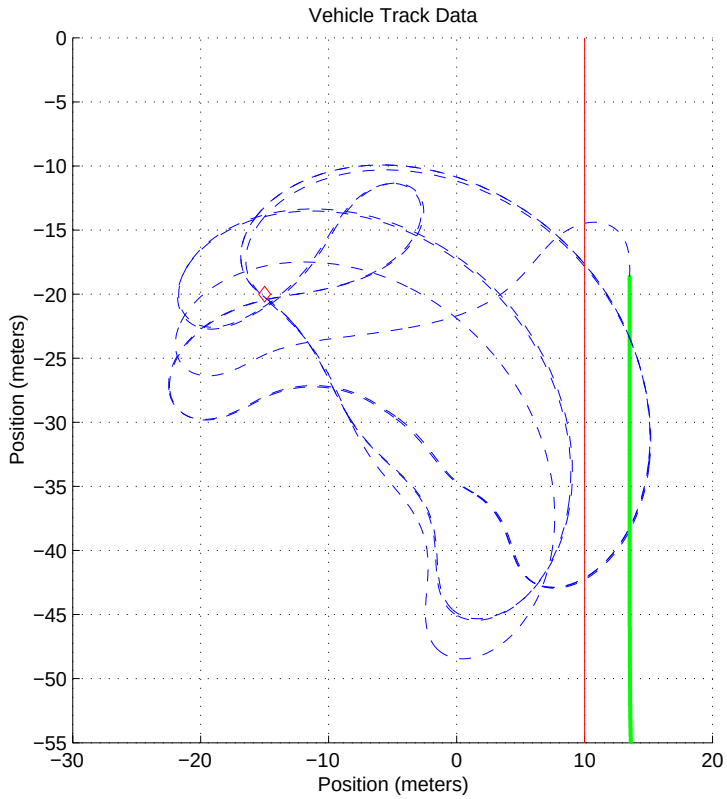

Figure 32. Loitering Track after 90 seconds with a SE Setting Current.

Figures 31 and 32 show that the vehicle continues to exhibit irregularities in the shape of the loitering track. The track above is a simulation of 90 second loitering time. The boundedness of the loitering is also increased to a diameter of approximately 38 meters.

6. Current Condition Simulation #6

Next the direction at which the AUV proceeded to the loiter point was changed so that the vehicle traveled into the current as it approached the loiter point. Figures 33 and 34 are the results.

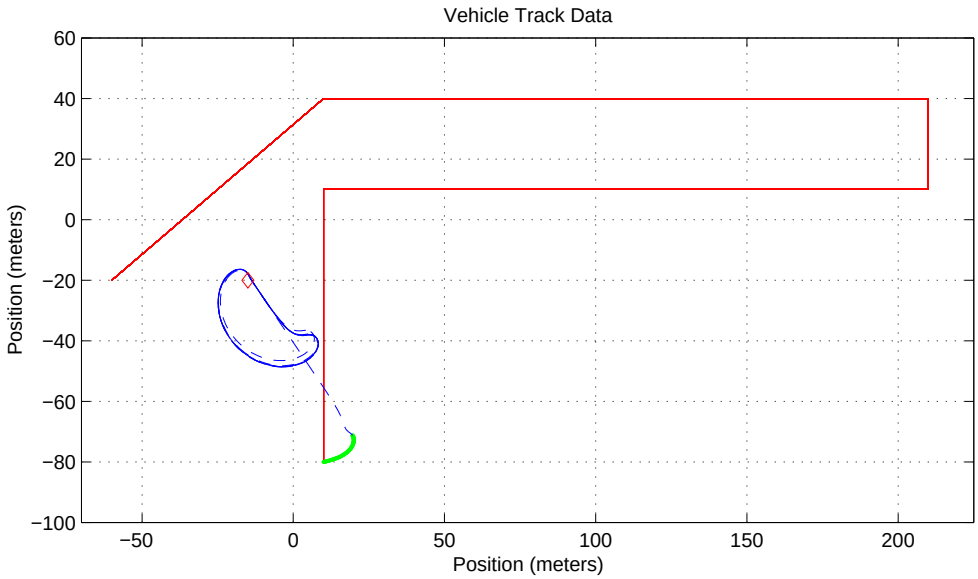

Figure 33. Loitering Track after 100 Seconds with a SE Setting Current.

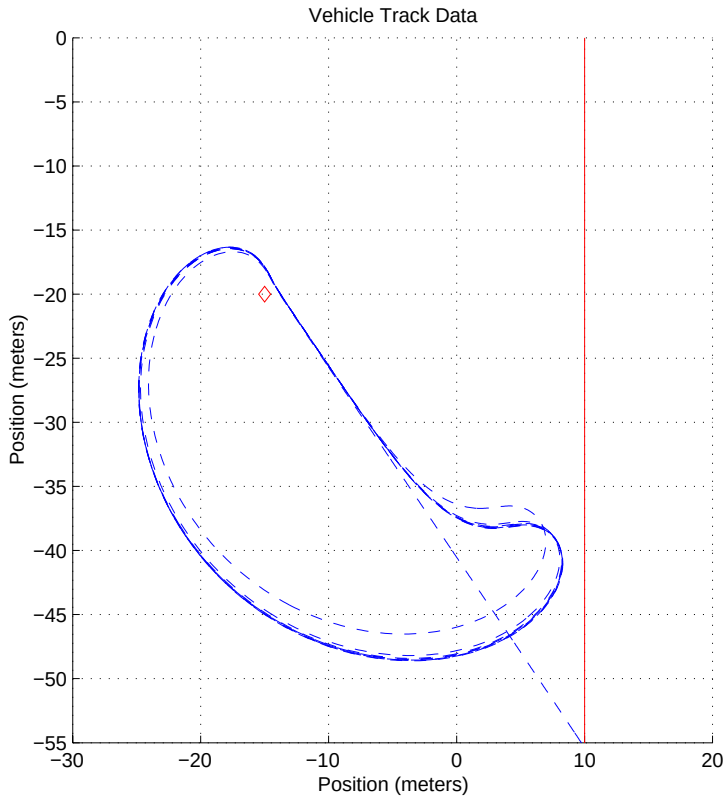

Figure 34. Loitering Track after 100 Seconds with a SE Setting Current.

From Figures 33 and 34 again it is observed that when the vehicle proceeds to the loiter point traveling against the current the loitering track shape is in a more predictable manner. In this case, the shape becomes more semi-circular with a bounded diameter of approximately 33 meters.

7. Current Condition Simulation #7

The current direction was changed to a Northeasterly direction and the vehicle was again ordered to the loiter point by traveling directly into the onsetting current. Figures 35 and 36 are the results.

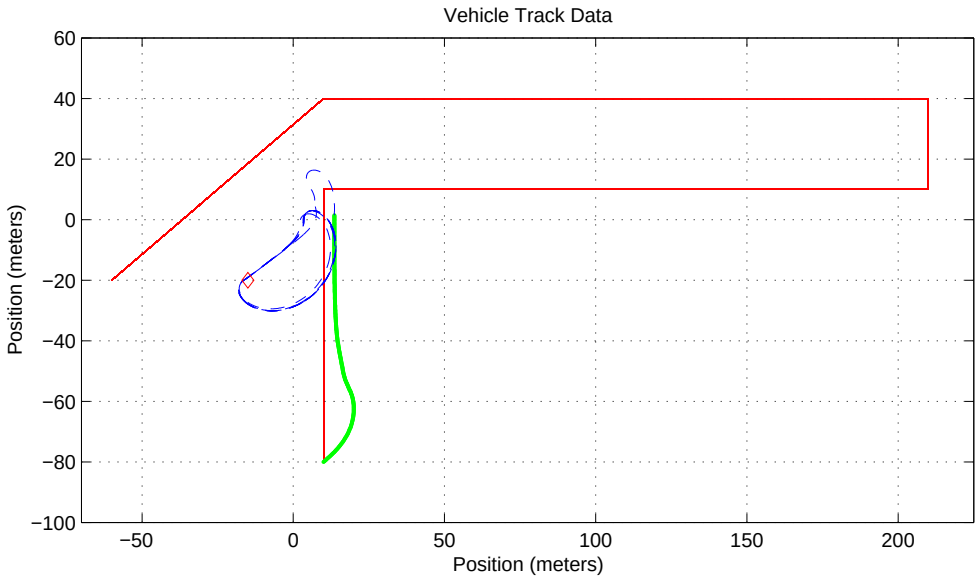

Figure 35. Loitering Track after 100 Seconds with a NE Setting Current.

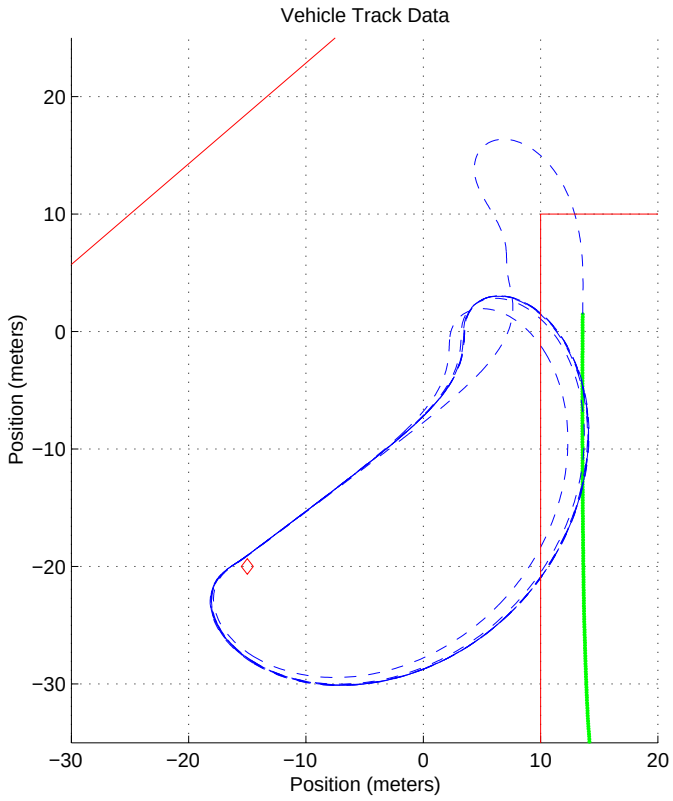

Figure 36. Loitering Track after 100 Seconds with a NE Setting Current.

Figures 35 and 36 again show that there is a relationship with the approach track to the loiter point and the current direction. The shape of the loitering track is semi-circular in nature and bounded with a diameter of approximately 33 meters as in Figures 33 and 34.

8. Current Condition Simulation #8

The current direction was changed to a Northwesterly direction and the vehicle proceeded with the current direction towards the loiter point. Figure 37 and 38 are the results.

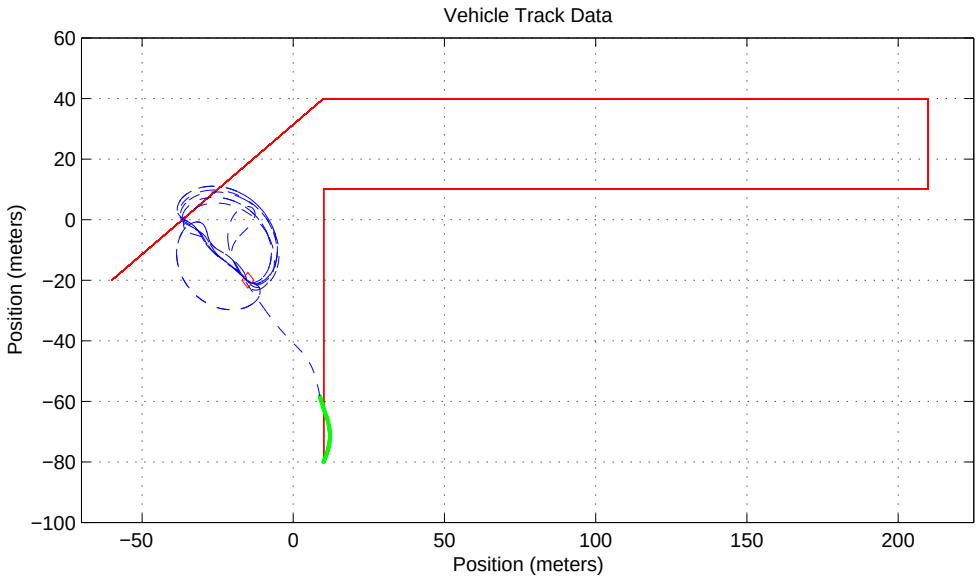

Figure 37. Loitering Track after 100 Seconds with a NW Setting Current.

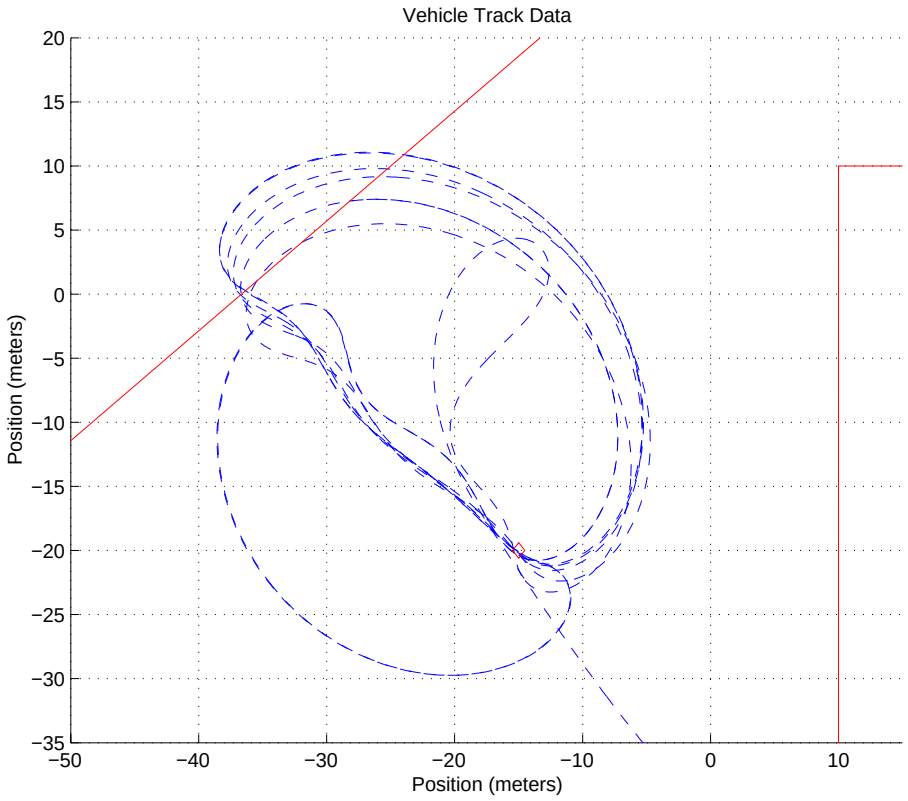

Figure 38. Loitering Track after 100 Seconds with NW Setting Current.

The characteristics of this track differ from the same approach that the AUV took in Figures 28 through 30 is that this pattern is not dominated by "figure 8" tracks, but rather an alternating semi-circular pattern. The pattern is still somewhat irregular in nature and the track is now bounded by approximately 42 meters in diameter.

V. DISCUSSION OF RESULTS

A. RELATION BETWEEN APPROACH AND CURRENT DIRECTION

From the simulations and data collected, it was observed that the track the vehicle traveled on during loiter is related to the position at where the vehicle was ordered to proceed to the loiter point and the direction of the current. If ARIES proceeds to a loiter point while traveling against the current, the shape of the loiter track is more predictable and regular and the bounded area is minimized.

The reason for this relationship lies within the Cross Track Error Controller of ARIES. When the vehicle is ordered to a loiter point, the heading directly to that position becomes the track heading of the vehicle. As the vehicle passes over the loiter point, the heading and steering controllers steer the vehicle in an attempt to regain the original track heading, therefore, the AUV "circles" the point. As the vehicle circles the loiter point, the current direction positions the AUV in such a manner that there is an ample distance to proceed on the original track heading towards the loiter point and the process is repeated. Figure 39 below is an illustration of what is being explained above. The vehicle is on an original heading of 000 deg T and the current direction is 180 deg T. As the vehicle passes over the loiter point, the controllers direct the vehicle is such a manner so that it regains the 000 deg T track as it approaches the loiter point. The current direction assists the controllers by setting the vehicle far enough away from the loiter point that it can settle out on the 000 deg T leg.

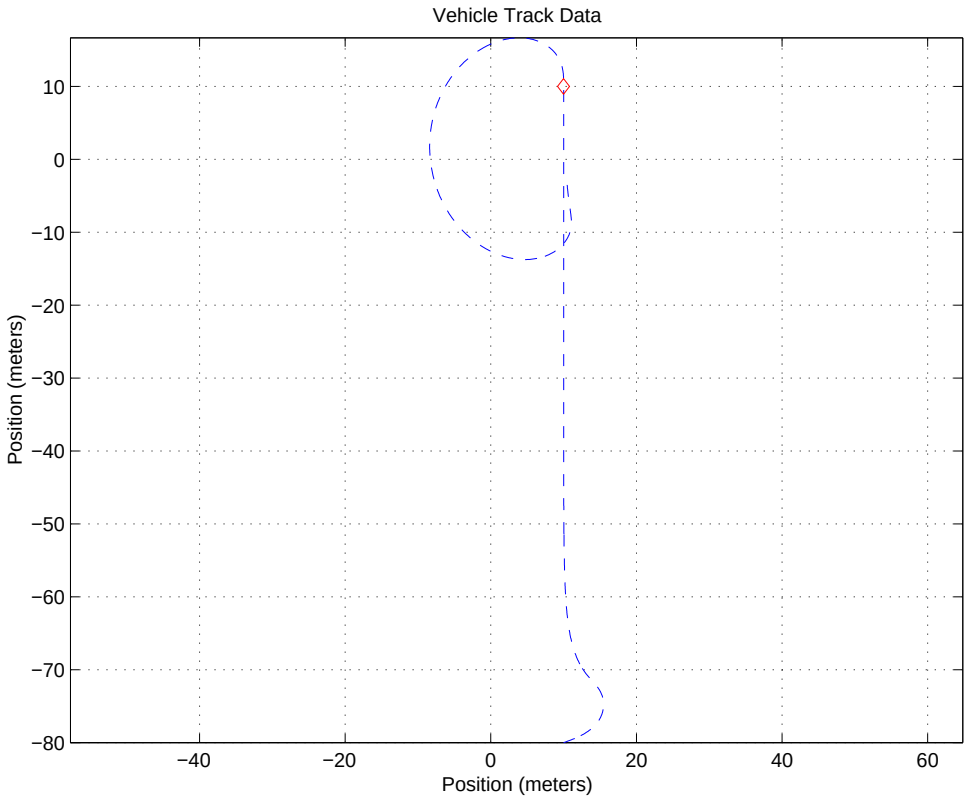

Figure 39. Relation of Vehicle Approach and Current Direction.

B. LINE OF SIGHT GUIDANCE INSTABILITY

Since there is a relationship between the Cross Track Error Guidance and the current direction, an analysis of using Line of Sight Guidance only during a loiter was conducted. The vehicle does not need to get to the loiter station by a straight line using Cross Track Error, it just needs to maintain a predictable and tight track pattern. A simple simulation was run with the AUV using Line of Sight Guidance only during a loiter and the results can be seen in Figure 40 below.

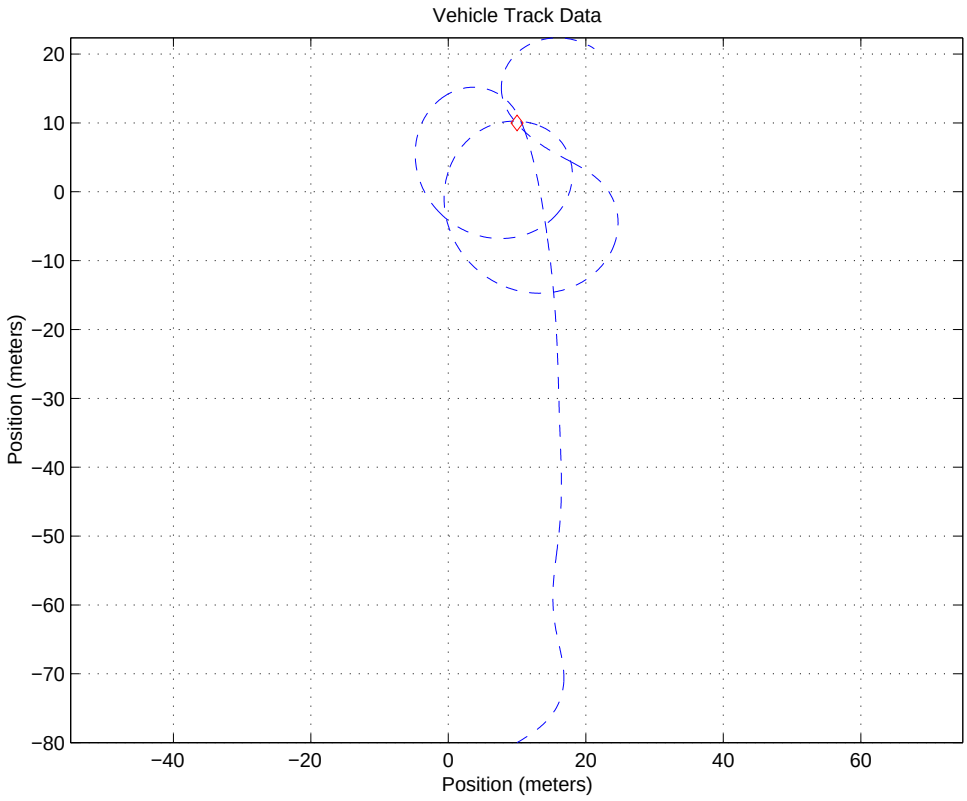

Figure 40. Line of Sight Guidance only during a loiter with no current.

Figure 40 shows that with Line of Sight Guidance only, the vehicle still has an erratic and unpredictable track pattern. So the stability of the Line of Sight Guidance was next analyzed thoroughly.

To analyze the stability of the Line of Sight Guidance the closed loop matrix of the system was calculated. To calculate this the following was solved:

$$\begin{bmatrix} \dot{v} \\ \dot{r} \\ \dot{\psi} \\ \dot{Y} \end{bmatrix} = (M^{-1}A)\begin{bmatrix} v \\ r \\ \psi \\ Y \end{bmatrix} + (M^{-1}B)\delta_r \tag{24}$$

$$\text{where, } (M^{-1}A) = \begin{bmatrix} -0.1492 & 0.8895 & 0 \\ -0.0507 & -0.4109 & 0 \\ 0 & 1 & 0 \end{bmatrix}$$

and $(M^{-1}B) = \begin{bmatrix} 0.1533 \\ -0.1650 \\ 0 \end{bmatrix}$

leaving equation (24) looking like:

$$\begin{bmatrix} \dot{v} \\ \dot{r} \\ \dot{\psi} \\ \dot{Y} \end{bmatrix} = \begin{bmatrix} -0.1492 & 0.8895 & 0 & 0 \\ -0.0507 & -0.4109 & 0 & 0 \\ 0 & 1 & 0 & 0 \\ 0 & 0 & U & 0 \end{bmatrix} \begin{bmatrix} v \\ r \\ \psi \\ Y \end{bmatrix} + \begin{bmatrix} 0.1533 \\ -0.1650 \\ 0 \\ 0 \end{bmatrix} \delta_r$$

where, U is the forward speed of the vehicle and δ_r is incorporated from equation (9).

$$\delta_r = -k_1 v - k_2 r - k_3 \psi - k_4 \psi_{com};$$

where, $\psi_{com} = (\frac{d\psi}{dy})Y$ and therefore leaving δ_r as:

$$\delta_r = -k_1 v - k_2 r - k_3 \psi + k_3 (\frac{1}{s})Y$$

where, $k_1 = 0$ and k_2, k_3 are taken from equation (9).

$$k_2 = (-1.543)(2.5394)$$
$$k_3 = (-1.5)\frac{\eta}{\phi}\sigma$$

where, σ is solved from equation (8) and $\eta = 1.0$ and $\phi = 0.5$.

Now that δ_r is in terms of $\begin{bmatrix} v \\ r \\ \psi \\ Y \end{bmatrix}$, the A and B matrices can be combined in the form:

$$\begin{bmatrix} \dot{v} \\ \dot{r} \\ \dot{\psi} \\ \dot{Y} \end{bmatrix} = [A - Bk] \begin{bmatrix} v \\ r \\ \psi \\ Y \end{bmatrix}$$

where, $[A - Bk]$ is the closed loop matrix, A_c, of the system. The eigenvalues of A_c were found and plotted against the distance to the loiter point, s. Figure 41 below shows the results.

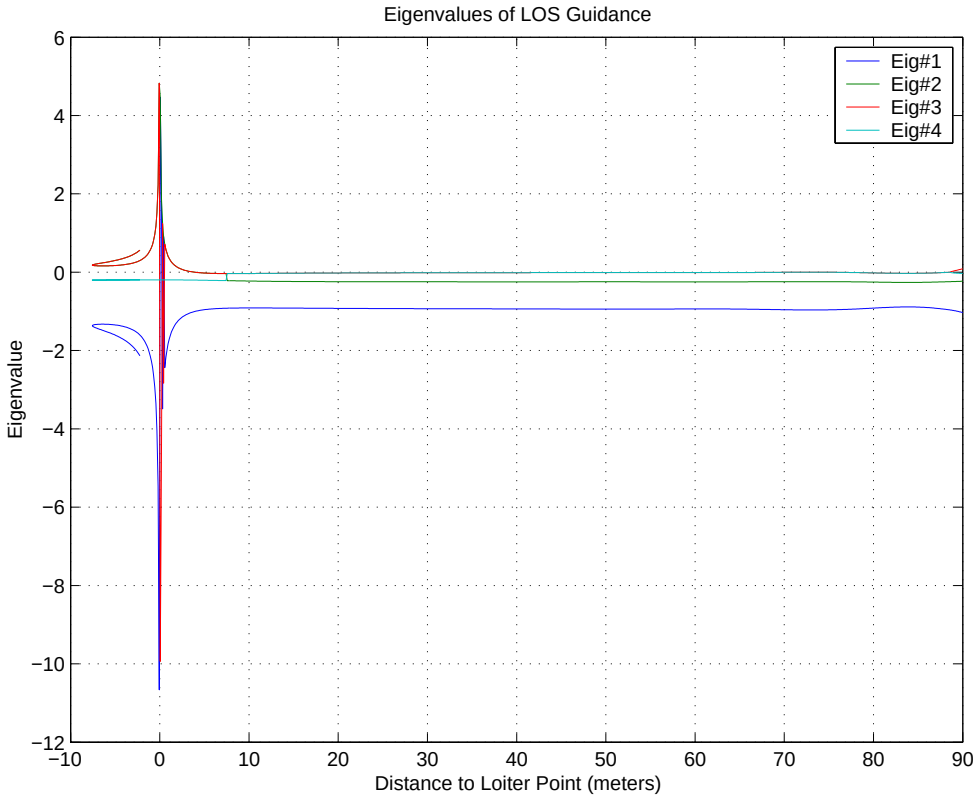

Figure 41. Eigenvalues of LOS Guidance.

Figure 41 shows that the LOS Guidance system is stable farther away than close in. The system goes unstable in this scenario approximately 3.9 meters from the loiter point. Figure 42 is a closer look at the position at where the system goes unstable with an Eigenvalue crossing the zero axis.

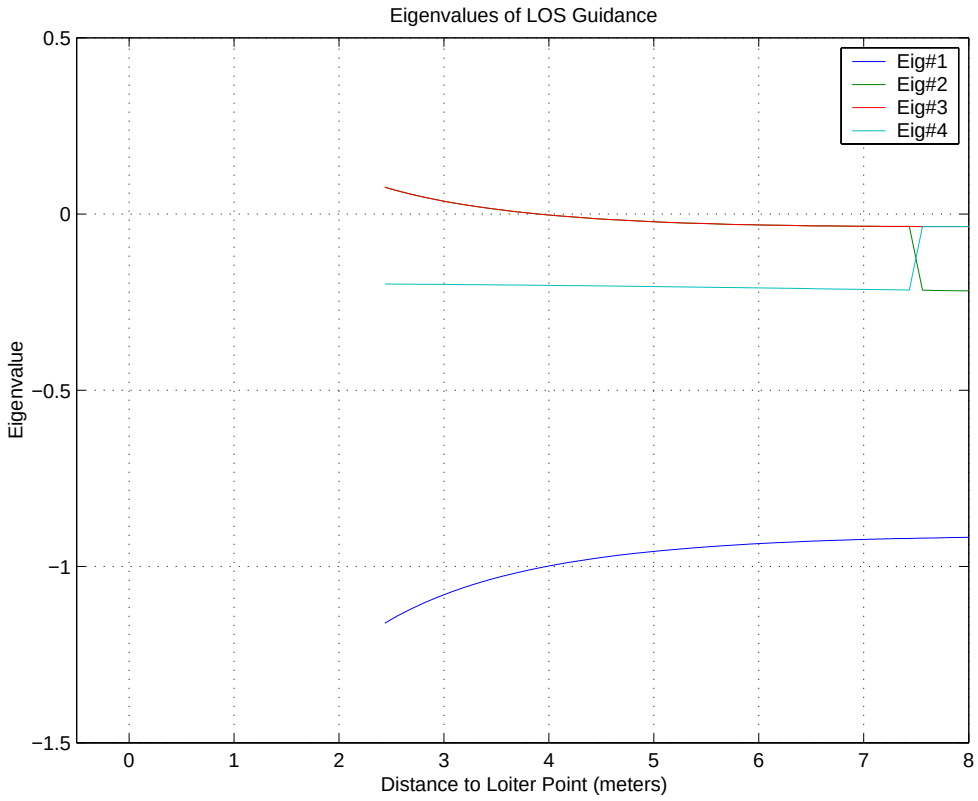

Figure 42. Close In View where Eigenvalues of LOS Guidance Go Unstable.

Figures 41 and 42 explain the vehicle's tendencies to be stable when it is a greater distance away than when the vehicle is closer in. Under normal operations when the vehicle is following a pre-programmed track with no loiter points, the stability of the Line of Sight Guidance never becomes a problem because the watch radius around the transition points or way points is usually set to approximately 10 meters. Therefore, the AUV transitions to the next way point without the Line of Sight Guidance going unstable. But when a loiter point is introduced into the program, the vehicle generally cannot maintain a steady and predictable shape, but rather a random, unpredictable track due to the instability of the Line of Sight Guidance.

VI. STABILITY ANALYSIS

A. LIAPUNOV STABILITY/INSTABILITY THEOREMS

To investigate the instability of the Line of Sight Guidance even further, the theorems of Liapunov were employed. Stability in the sense of the theories from Liapunov is concerned with the behavior of a system in the vicinity of an equilibrium state. Liapunov stated that if there exists a positive-definite function V(x) that is never increasing, the origin is stable [8]. In this case, the origin is the loiter point.

In mathematical terms, the Liapunov Stability Theorem states if there exists a continuously differentiable function V(x) such that:

1. V(0) = 0
2. V(x) > 0 for all $x \neq 0$
3. $\frac{dV}{dt} = (\frac{\partial V}{\partial x})' f(x) = \sum_{i=1}^{n} \frac{\partial V}{\partial x_i} f_i(x) \leq 0$ for all x

then the origin of the time-invariant system

$$\dot{x} = f(x)$$

is stable.

Liapunov's Instability Theorem states that if there exists a positive-definite function V(x) whose derivative $\dot{V}$ (x) is non-negative in a region containing the origin, then the origin is unstable.

Applying this theory, a MATLAB program was created to compare the Liapunov's Stability/Instability Theorems to the loitering motions of the ARIES where a Liapunov function was chosen and V versus $\dot{V}$ was plotted.

The program has the vehicle starting at a point very close to the origin, which is the loitering station and the Liapunov function is $V = (x-10)^2 + (y-10)^2$. There are no current conditions and Line of Sight Guidance is only used. Figures 43 and 44 below

provide proof through Liapunov's Stability and Instability Theorems that the AUV's Line of Sight Guidance becomes unstable when it gets close to the origin (loiter point).

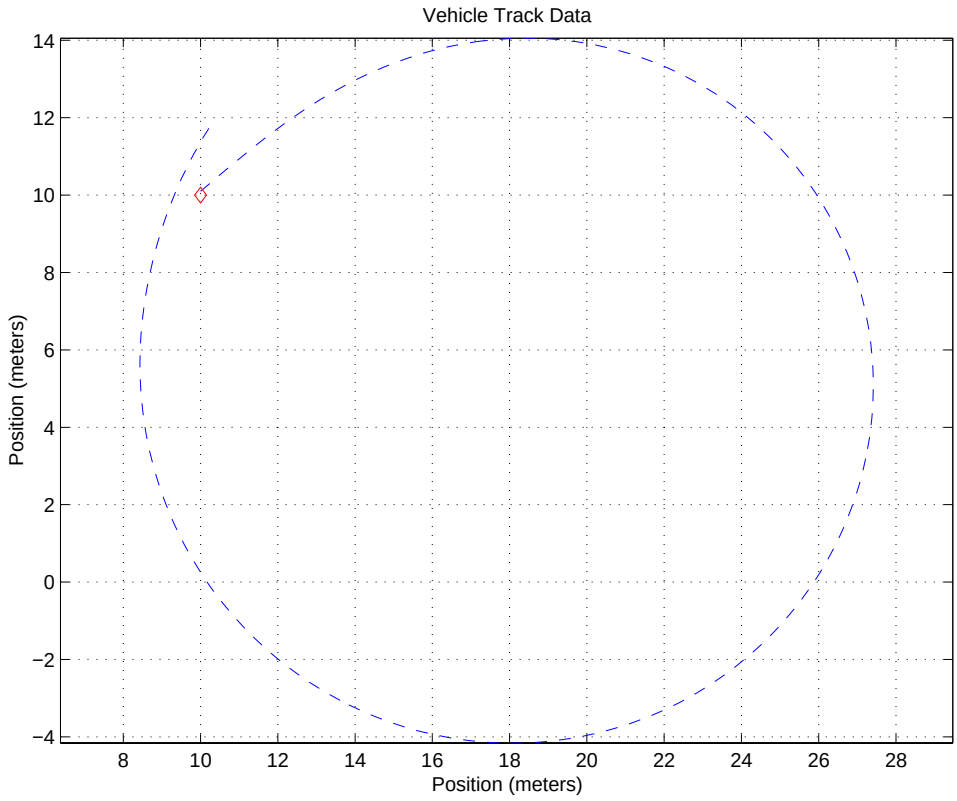

Figure 43. Vehicle Track Data of ARIES.

Figure 43 starts the AUV very close to its loiter point and the vehicle begins a series of right turns to attempt to reach its programmed way point or loiter point in this case. Figure 44 below shows how the Line of Sight Guidance is stable as it begins to track into the point at a greater distance away, but then goes unstable when it gets a few meters from the point.

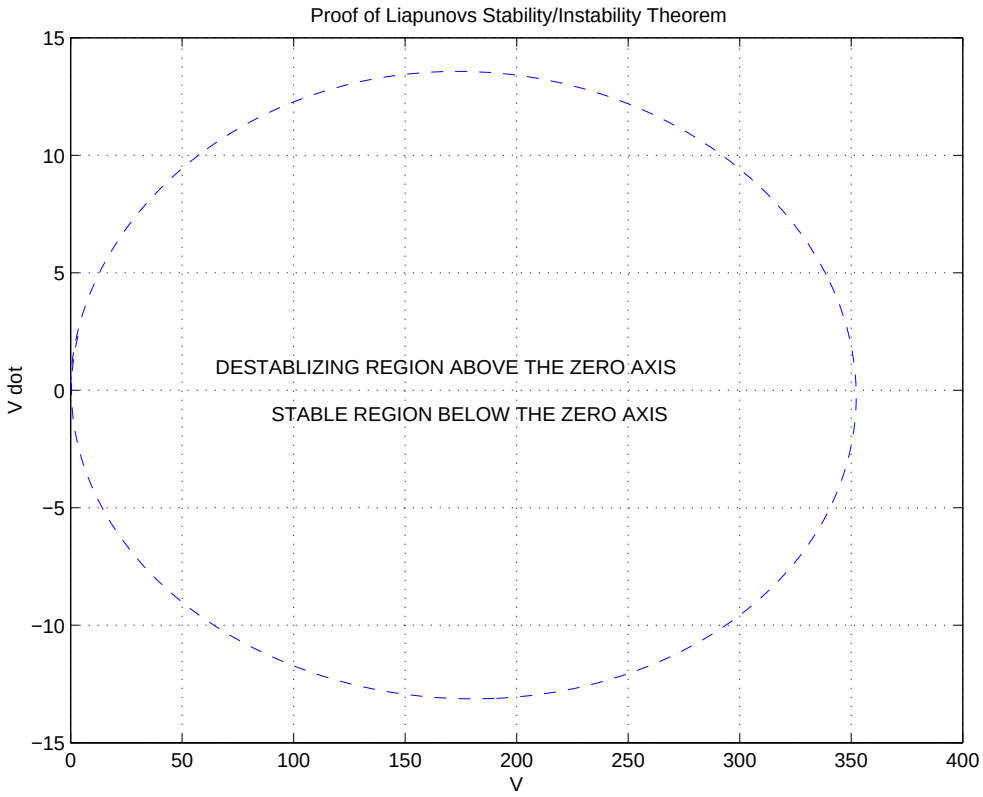

Figure 44. V dot versus V.

THIS PAGE INTENTIONALLY LEFT BLANK

VII. CONCLUSIONS AND RECOMMENDATIONS

Although the loitering track of the ARIES is not predictable in most cases, the loitering track of the vehicle is a bounded region for all cases. If a situation arises where ARIES is required to maintain a circular pattern on a point or loiter station with no deviation in its track, then a series of way points constructed in a circular, octagon, or box pattern can be constructed and the vehicle will follow these points. This technique has been proven through experiments run with the vehicle in previous missions.

Shutting the vehicle off at a loiter point is not an option for the following reasons. Ultimately the AUV will operate in potentially hostile waters. If the vehicle is shut off at its loiter station, the AUV will automatically surface making itself susceptible to enemy detection and ultimately compromising its mission. Also, since the AUV is surfaced it will still be effected by current conditions and will not maintain position on the loiter point.

ARIES is constructed to be equipped with lateral and vertical thrusters. A hovering control law algorithm could be constructed that would utilize the thrusters in the vehicle's attempt to maintain station on one point. This would prove to be useful because the instability of the Line of Sight Guidance would not come into play if such a control law existed, however, more power would be consumed in the process.

THIS PAGE INTENTIONALLY LEFT BLANK

APPENDIX A. *MATLAB* FILES FOR AUV LOITERING

The *MATLAB* code associated and developed for loitering behavior is contained on CD-ROM and is obtainable through request from Professor A.J. Healey. This appendix contains the *MATLAB* script file for the ARIES AUV to loiter and continue on original track if desired. Currents can be introduced if desired.

- LoiterToTrackRun.m

THIS PAGE INTENTIONALLY LEFT BLANK

APPENDIX B. *MATLAB* FILES FOR AUV LOITERING

The *MATLAB* code associated and developed for loitering behavior is contained on CD-ROM and is obtainable through request from Professor A.J. Healey. This appendix contains the *MATLAB* script file for a simple approach to loiter for the ARIES AUV.

- simpleloiter.m

THIS PAGE INTENTIONALLY LEFT BLANK

APPENDIX C. *MATLAB* FILES FOR AUV LOITERING

The *MATLAB* code associated and developed for loitering behavior is contained on CD-ROM and is obtainable through request from Professor A.J. Healey. This appendix contains the *MATLAB* script file for a simple approach to loiter for the ARIES AUV using Line of Sight Guidance only. The eigenvalues of the closed loop LOS Guidance are plotted versus distance to the loiter point to show instability.

- LOSinstability.m

THIS PAGE INTENTIONALLY LEFT BLANK

APPENDIX D. *MATLAB* FILES FOR AUV LOITERING

The *MATLAB* code associated and developed for loitering behavior is contained on CD-ROM and is obtainable through request from Professor A.J. Healey. This appendix contains the *MATLAB* script file to show the relationship between Liapunov's Stability/Instability Theorem to LOS Guidance.

- Reverseinstability.m

THIS PAGE INTENTIONALLY LEFT BLANK

LIST OF REFERENCES

[1] Marco, D.B., Healey, A.J., "Command, Control, and Navigation Experimental Results With the NPS Aries AUV", IEEE Journal of Oceanic Engineering , v.26, n.4, Oct. 2001, pp.466-476.

[2] Ashtech Products, G12 Sensor, http://ashtech.com/Pages/prodoem.htm.

[3] L. R. LeBlanc, M. Singer, P. Beaujean, et. Al., "Improved Chirp FSK Modem for High Reliability Communications in Shallow Water", Proceedings IEEE Oceans 2000, IEEE #00CH37158C, pp. 601-603, 2000.

[4] Healey, A.J., Lienard, D., "Multivariable Sliding Mode Control for Autonomous Diving and Steering of Unmanned Underwater Vehicles", IEEE Journal of Oceanic Engineering, v.18, n.3, July 1993, pp.1-13.

[5] Genon, G., An, E.P., Smith, S.M., Healey, A.J., "Enhancement of the Inertial Navigation System for the Morpheous Autonomous Underwater Vehicles", IEEE Journal of Oceanic Engineering, v.26, n.4, Oct. 2001, pp.548-560.

[6] Healey, A.J., An, E.P., Marco, D.B., "On Line Compensation of Heading Sensor Bias for Low Cost AUV Navigation", Proceedings of IEEE AUV '98, Cambridge, Mass, Aug. 20-21, 1998.

[7] Cassandras, C.G., 1993, "Discrete Event Systems, Modeling and Performance Analysis", Irwin-Aksen , ISBN-0-256-11212-6.

[8] Friedland, B., 1996, "Advanced Control System Design", Prentice-Hall, ISBN-0-13-0140104.

THIS PAGE INTENTIONALLY LEFT BLANK

INITIAL DISTRIBUTION LIST

1. Defense Technical Information Center
   Ft. Belvoir, VA 22060-6218

2. Dudley Knox Library
   Naval Postgraduate School
   Monterey, CA

3. Mechanical Engineering Department Chairman, Code ME
   Naval Postgraduate School
   Monterey, CA

4. Naval/Mechanical Engineering Curriculum Code 34
   Naval Postgraduate School
   Monterey, CA

5. Professor Anthony J. Healey, Code ME/HY
   Department of Mechanical Engineering
   Naval Postgraduate School
   Monterey, CA

6. Dr. Donald Brutzman, Code UW/Br
   Undersea Warfare Group
   Naval Postgraduate School
   Monterey, CA

7. Dr. T. B. Curtin, Code 322OM
   Office of Naval Research
   Arlington, VA

8. Dr. T. Swean, Code 32OE
   Office of Naval Research
   Arlington, VA

9. LT Douglas L. Williams
   Strategic Systems Program
   Kings Bay, GA

10. LT Joe Keller
    Naval Postgraduate School
    Monterey, CA

11. LT Lynn Fodrea
Naval Postgraduate School
Monterey, CA